The Fiscal Costs of Climate Change in the United States
Online Appendix

Lint Barrage
ETH Zurich

August 2026

Contents

A1 Empirical Analysis

A1.1 Further Results - Robustness

A1.1.1 Inclusion of Covid Years

The benchmark analysis excludes data from the Covid pandemic years 2020-2022 due to concerns over undue influence of unusual healthcare expenditure patterns from this time period. Table $A1$ repeats the main specification with the Covid years included. The results suggest slightly larger effects of extreme heat.

A1.1.2 Spatio-Temporal Controls

This section showcases the robustness of the empirical results to alternative spatio-temporal controls. Column 1 of Table $A2$ replicates the preferred benchmark specification from Table 1 Column 1. Column 2 shows that the results are robust to clustering standard errors at the state- instead of the county-level.[1] Columns 3 and 4 show that the results are also similar when time trends are switched from linear state-level trends to quadratic state-level or linear county-level trends, respectively. Finally, Column 5 shows results without any socio-economic controls, for which marginal heat impacts appear slightly larger but ultimately of a similar magnitude to the benchmark. As the goal of our estimation is to create an input to a structural model that accounts separately for population and income dynamics (including climate impacts on income levels), our preferred empirical specification holds socio-economic variables constant to estimate a ceteris paribus impact on public health expenditures. Finally, we note that aggregating all data to the state-year level and performing an equivalent estimation yields coefficients that are similar in magnitude but no longer precisely estimated (not shown).

[1] Interestingly, the standard errors on the heat days are even slightly smaller in this specification, as can occur (Cameron and Miller 2015) and has been found in other recent U.S. health studies (e.g., Larsen et al. 2023).

Table A1: Robustness: Including Covid Years (2020-2022)

Dep. Var.:	ln(Public Medical Expenditures/Pop.)				
	(1)	(2)	(3)	(4)	(5)
Extreme Heat Days$_{j,t}$	0.00529***	0.00650***	0.00139***	0.00020*	0.00020**
	(0.00114)	(0.00154)	(0.00018)	(0.00011)	(0.00009)
Extreme Heat Days$_{j,t}$ $\times$ $\overline{T}_{m,j}$	-0.00022***	-0.00027***	-0.00002**	0.00000	
	(0.00006)	(0.00008)	(0.00001)	(0.00000)	
Pop-weighted Avg. MFX$_{\text{Extreme Heat}}$	0.0021	.0022	.0013	.0002	.0002
Freezing Days$_{j,t}$	0.00016	-0.00005	-0.00026**	0.00009	-0.00022**
	(0.00017)	(0.00019)	(0.00012)	(0.00014)	(0.00009)
Freezing Days$_{j,t}$ $\times$ $\overline{T}_{m,j}$	-0.00001	-0.00003*	0.00000***	0.00000	
	(0.00001)	(0.00001)	(0.00000)	(0.00000)	
Pop-weighted Avg. MFX$_{\text{Freezing}}$	-.00000	-.00008	-.0001	.0001	-0.0002
Obs.	79,403	79,403	79,403	79,403	79,403
Adj. R-Sq.	0.971	0.971	0.971	0.971	0.971
#Counties (Clusters)	3,055	3,055	3,055	3,055	3,055
"Heat" Measure	Avg.>32C	Avg.>32C	Avg.>32C	Max.>35C	Avg.>97.5th Pct.
"Freezing" Measure	Avg.<0C	Avg.<0C	Avg.<0C	Min.<0C	Avg.<2.5th Pct.
$\overline{T}_{m,j}$ is average of:	Temp.	Temp.	#H/F Days	#H/F Days	-
Demo./Inc./Precip./Hurricane Controls:	Yes	Yes	Yes	Yes	Yes
Precip. $\times$ Hot, Cold	No	Yes	No	No	No
County F.E.s:	Yes	Yes	Yes	Yes	Yes
Year F.E.s:	Yes	Yes	Yes	Yes	Yes
State-Trends:	Yes	Yes	Yes	Yes	Yes

Table shows results of linear regression of log of county-year public medical expenditures per capita (1996-2022, from BEA) on the number of "heat" days (defined as avg. daily temp.>32C in Cols 1-3, max. daily temp.>35C in Col. 4, avg. daily temp.>97.5th county pctl. in Col 5), "freezing" days (defined as avg. daily temp.<0C in Cols 1-3 and min. daily temp.<0C in Col. 4, avg. daily temp.<2.5th pctl. in Col 5.) both in levels and interacted with climate measures $\overline{T}_{m,j}$ (avg. temp. in Cols. 1-2 and avg. number hot/cold days in Cols. 3-4) (based on data from PRISM) along with county fixed effects, linear state-level trends, year fixed effects and controls for log of county pop., log of the population 65 years and older, prior to current year population growth, percent non-hispanic whites (from the National Center for Health Statistics), log and growth of real per capita income (from BEA), precipitation (2nd order polynominal) plus interaction of precipitation and "heat"/"freezing" days in Col. 2 (based on data from PRISM), and the number of hurricane days in the county-year (NOAA Storm Events Database). Regressions are weighted by county populations. Standard errors are heteroskedasticity-robust and clustered at the county level. P-values are labeled: *** p<0.01, ** p<0.05, * p<0.1

A1.1.3 Finer Temperature Bins

The analysis thus far considers three temperature bins: very cold, very hot, and the interim (omitted) moderate temperature range. This section shows results for several versions of the benchmark regressions with finer temperature bins, specifically $4°C$ bins ranging from $(-\infty, -8°]$, $(-8°, -4°]$, ... $(28°, 32°]$, $(32°, 36°]$, $(36°, \infty)$, with (12,16] the omitted category. One caveat for the

Table A2: Robustness: Spatio-Temporal Controls

Dep. Var.:	ln(Public Medical Expenditures/Pop.)				
	(1)	(2)	(3)	(4)	(5)
Extreme Heat Days$_{j,t}$	0.00394***	0.00394***	0.00330*	0.00323***	0.00750***
	(0.00120)	(0.00081)	(0.00175)	(0.00105)	(0.00155)
Extreme Heat Days$_{j,t}$ $\times$ $\overline{T}_{m,j}$	-0.00015**	-0.00015***	-0.00013	-0.00012**	-0.00035***
	(0.00007)	(0.00004)	(0.00010)	(0.00006)	(0.00008)
Pop-weighted Avg. MFX$_{\text{Extreme Heat}}$	0.0018	0.0018	0.0015	0.0015	0.0025
Freezing Days$_{j,t}$	0.00029	0.00029	0.00063***	0.00009	0.00005
	(0.00019)	(0.00040)	(0.00018)	(0.00019)	(0.00019)
Freezing Days$_{j,t}$ $\times$ $\overline{T}_{m,j}$	-0.00003**	-0.00003	-0.00005***	-0.00001	-0.00001
	(0.00001)	(0.00003)	(0.00001)	(0.00001)	(0.00001)
Pop-weighted Avg. MFX$_{\text{Freezing}}$	-0.0001	-0.0001	-0.0001	-0.0000	-0.0000
Obs.	70,239	70,239	70,239	70,239	73,338
Adj. R-Sq.	0.972	0.972	0.975	0.985	0.959
SE-Clustering:	County	State	County	County	County
Socio-Economic Controls:	Yes	Yes	Yes	Yes	No
Time Trends:	State, Linear	State, Linear	State, Quadratic	County, Linear	State, Linear

Table shows results of linear regression of log of county-year public medical expenditures per capita (1996-2019, from BEA) on the number of "heat" days (defined as avg. daily temperature>32C), "freezing" days (defined as avg. daily temperature<0C) both in levels and interacted with avg. long-run temperature $\overline{T}_{m,j}$ (based on data from PRISM) along with county fixed effects, year fixed effects, linear time trends at the state- (Cols. 1, 2) or county- (Co. 4) level, or quadratic trends at the state level (Col. 3), plus in Cols. 1-4 controls for log of county populations, log of the population 65 years and older, prior to current year population growth, percent non-hispanic whites from the National Center for Health Statistics), log and growth of real per capita income (from BEA). All control for precipitation (2nd order polyn.) and number of hurricane days in county-year (NOAA Storm Events Database). Regressions weighted by county populations. Standard errors are heteroskedasticity-robust and clustered at the county level (Cols. 1, 3, 4, 5) or at the state level (Col. 2). P-values are labeled: *** p<0.01, ** p<0.05, * p<0.1

higher temperature bins is that days with 24-hour *average* temperatures above $32°C$ are already extreme events, with the average county experiencing only 0.71 such days per year. Cutting this variation more finely into county-days with higher average temperatures thus limits the available variation in the data and makes estimated effects vulnerable to noise from outlier effects. For example, only 226 counties ever experience a day where 24-hour average temperatures exceed $36°C$.

Figures A1-A3 show results from estimating the finer binned impacts for the benchmark specification of Table 1 Column 1 in the full sample, the pre-Covid sample, and the Table 1 Column 3 specification in the pre-Covid sample, respectively. The specifications differ by whether local climate is measured by long-run average temperature (Col. 1) or the number of days a county on average experiences in each temperature bin (Col. 3). Marginal effects are displayed for the *average* county.

The results confirm that the most important temperature categories with regards to detectable aggregate public health expenditure impacts in our sample are indeed the extreme cold and extreme heat days. Days with average temperatures in the $(32°, 36°]$ bin are consistently associated with economically and statistically significant increases and public health expenditures. While the results also reveal the possibility of statistically significant impacts in some lower temperature bins, these are generally an order of magnitude smaller than the extreme heat day effects and less robustly estimated. Finally, estimated impacts of the most extreme heat category $(36°, \infty)$ are imprecise and sensitive to specification, as may be expected given their limited extent in the data.

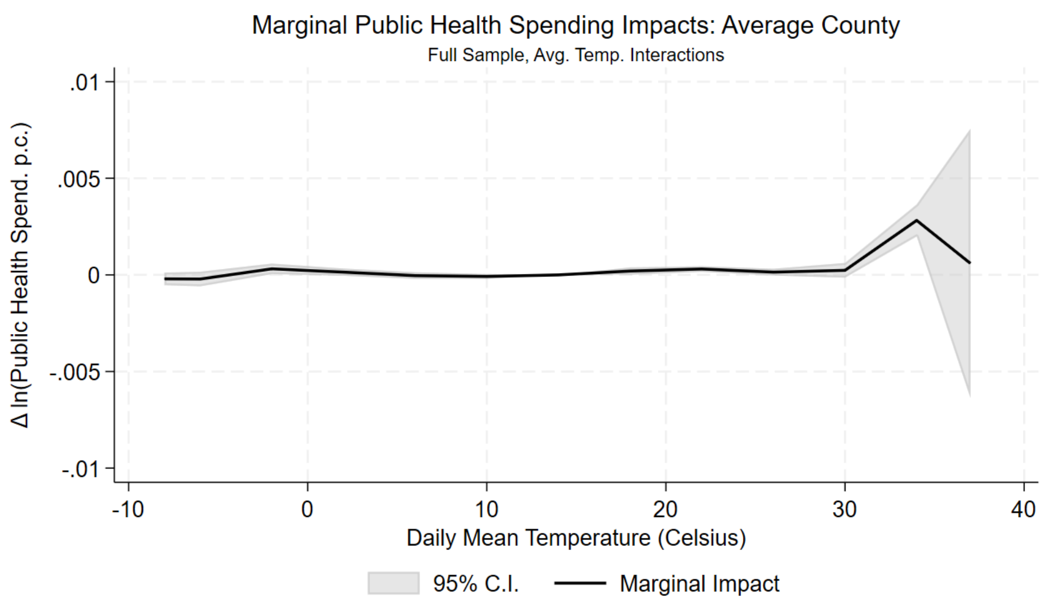

Figure A1

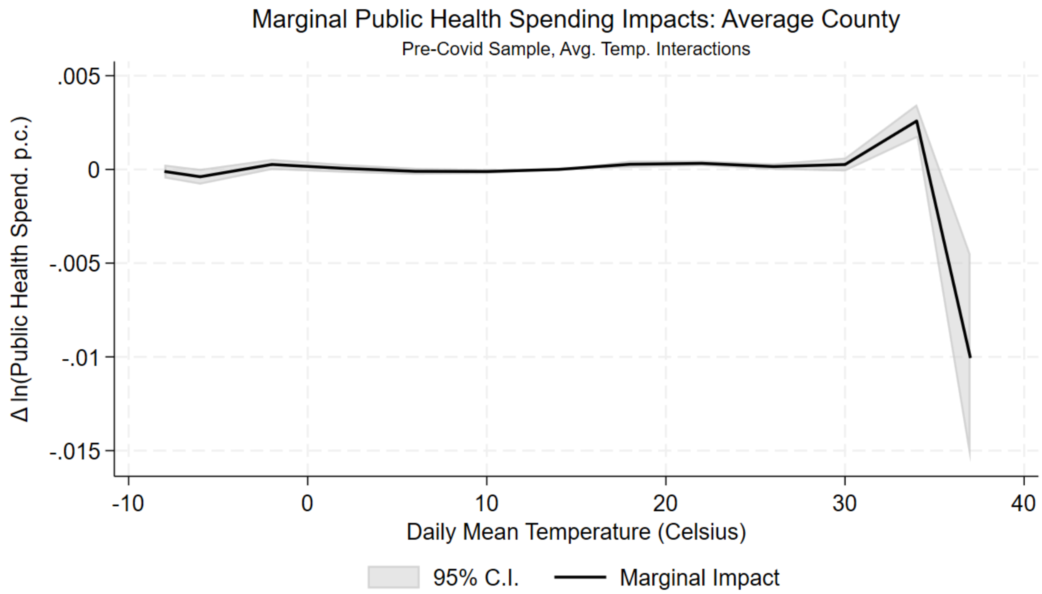

Figure A2

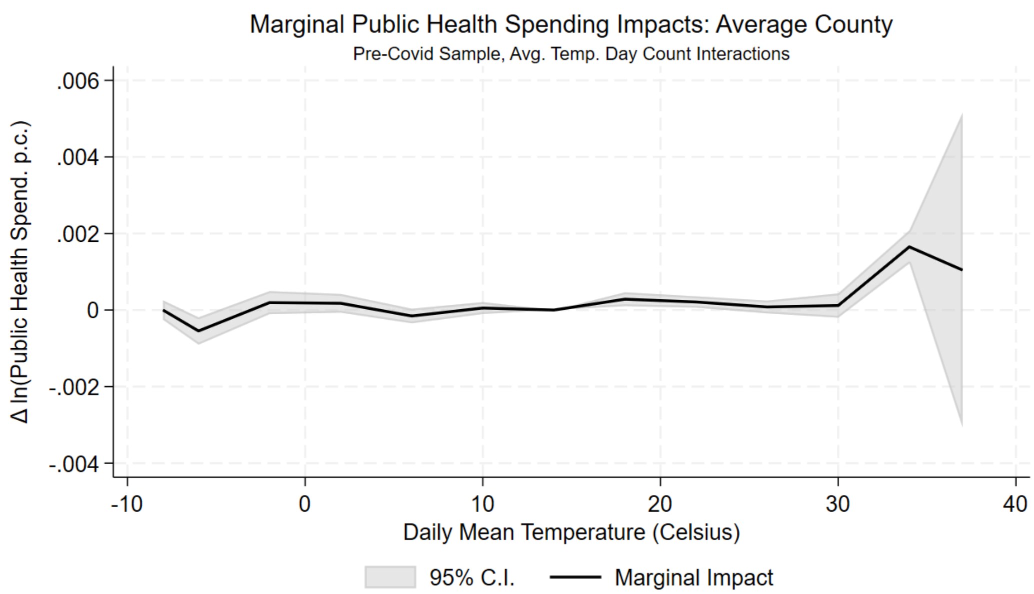

Figure A3

A1.1.4 Income Interactions

The benchmark analysis averages the responsiveness of public health expenditures to weather conditions across income levels. This section considers heterogeneity in the marginal effects based on income. Conceptually, while higher income levels have been associated with lower *mortality* effects of temperature extremes (e.g., Carleton et al. 2022), it is less clear what to expect for health expenditures which reflect not only physical vulnerability but also depend on public health program availability and generosity, which have increased substantially with rising income levels in the United States, as illustrated in Figure A4 below. (In case this figure raises concerns about trends we would like to highlight that our analysis controls for state-specific trends in healthcare expenditures as well as aggregate time fixed effects.) Increasing responsiveness of adaptation-like climate impacts with higher incomes have also been observed, e.g., for energy consumption (e.g., Rode et al. 2021). On net, the empirical results suggest that the responsiveness of public healthcare costs to both extreme heat and cold days is significantly *increasing* in local income levels. Using these results in our future fiscal cost projections would thus, ceteris paribus, lead to *larger* estimates as U.S. incomes continue to rise. That is, while the average marginal effect of heat on public spending may appear slightly smaller in Table $A3$ compared to the benchmark, this average also reflects the evaluation at past income levels which are lower than current and future income levels. Conceptually, however, incorporating this positive income effect seems inconsistent with the preferred baseline assumption that U.S. government program generosity will remain at current levels. While our benchmark analysis thus does not incorporate a positive income effect, it should be acknowledged that this assumption may well bias future healthcare cost impact projections downward.

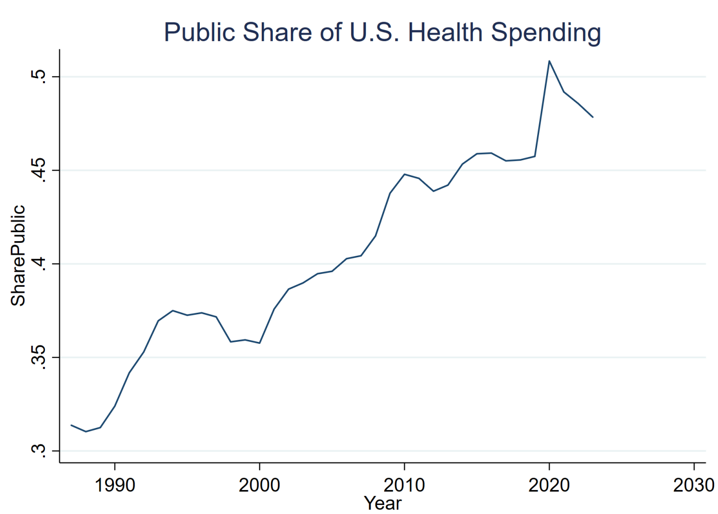

Figure A4: Share of public in total U.S. health spending over time (Data source: Peterson-KFF 2025)

Table A3: Robustness: Income Interactions

Dep. Var.:	ln(Public Medical Expenditures/Pop.)			
	(1)	(2)	(3)	(4)
Extreme Heat Days$_{j,t}$	-0.01957*	-0.01886*	-0.02172**	-0.02169***
	(0.01031)	(0.01056)	(0.00870)	(0.00422)
Extreme Heat Days$_{j,t}$ $\times$ $\ln(\text{p.c.Inc})_{m,t}$	0.00205**	0.00206**	0.00216***	0.00205***
	(0.00088)	(0.00086)	(0.00082)	(0.00040)
Extreme Heat Days$_{j,t}$ $\times$ $\overline{T}_{m,j}$	-0.00006	-0.00010	-0.00001*	0.00000*
	(0.00008)	(0.00010)	(0.00001)	(0.00000)
Pop-weighted Avg. MFX$_{\text{Extreme Heat}}$	0.0014	0.0014	0.0013	0.0002
Freezing Days$_{j,t}$	-0.00717***	-0.00680***	-0.00803***	-0.01142***
	(0.00253)	(0.00253)	(0.00247)	(0.00272)
Freezing Days$_{j,t}$ $\times$ $\times$ $\ln(\text{p.c.Inc})_{m,t}$	0.00070***	0.00065***	0.00071***	0.00107***
	(0.00024)	(0.00024)	(0.00023)	(0.00025)
Freezing Days$_{j,t}$ $\times$ $\overline{T}_{m,j}$	-0.00003**	-0.00004***	0.00001***	0.00000
	(0.00001)	(0.00001)	(0.00000)	(0.00000)
Pop-weighted Avg. MFX$_{\text{Freezing}}$	-0.0001	-0.0002	-0.0002	0.0001
Obs.	70,239	70,239	70,239	70,239
Adj. R-Sq.	0.972	0.972	0.972	0.973
#Counties (Clusters)	3,055	3,055	3,055	3,055
"Heat" Measure	Avg.>32C	Avg.>32C	Avg.>32C	Max.>35C
"Freezing" Measure	Avg.<0C	Avg.<0C	Avg.<0C	Min.<0C
$\overline{T}_{m,j}$ is average of:	Temp.	Temp.	#Heat/Freeze Days	#Heat/Freeze Days

Table shows results of linear regression of log of county-year public medical expenditures per capita (1996-2019, from BEA) on the number of "heat" days (defined as avg. daily temperature>32C in Cols 1-3 and max. daily temperature>35C in Col. 4), "freezing" days (defined as avg. daily temperature<0C in Cols 1-3 and min. daily temperature<0C in Col. 4) both in levels and interacted with climate measures $\overline{T}_{m,j}$ (avg. temp. in Cols. 1-2 and avg. number hot/cold days in Cols. 3-4) (based on data from PRISM) and log of per capita income $\ln(\text{p.c.Inc})_{m,t}$ (from BEA) along with county fixed effects, linear state-level trends, year fixed effects and controls for log of county populations, log of the population 65 years and older, prior to current year population growth, percent non-hispanic whites (from the National Center for Health Statistics), log and growth of real per capita income (from BEA), precipitation (2nd order polynominal) plus interaction of precipitation and "heat"/"freezing" days in Col. 2 (based on data from PRISM), and the number of hurricane days in the county-year (NOAA Storm Events Database). Regressions are weighted by county populations. Standard errors are heteroskedasticity-robust and clustered at the county level. P-values are labeled: *** p<0.01, ** p<0.05, * p<0.1

A1.1.5 Age Interactions

This section presents results for heterogeneous impacts by age, specifically by allowing the effects of both extreme heat and cold days to vary with the share of each county's population that is over 65 and below 5 years old, respectively. While prior literature has consistently found that *mortality* effects are concentrated among the elderly, emerging research shows that *morbidity* effects are quite different. Using hospital data from California, both White (2017) and Gould et al. (2025)

find that increases in emergency department visits on hot days are largest among <5 year olds, who account for 40% of excess visits but only 6% of the population. For hospitalization rates, both Gould et al. (2025) and Karlsson and Ziebarth (2018) also find increases across all age groups. Interestingly, for extreme cold, micro evidence points to very different age patterns: Gould et al. (2025) find that cold temperatures *decrease* emergency department visits among <5 year old but *increase* them among >65 year olds; Rizmie et al. (2022) similarly find *decreases* in risks of infectious disease and injuries among <5 year olds due to extreme cold but *increases* in both categories among >65 year olds. In line with all of the above, our analysis of aggregate annual health expenditures reveals larger impacts of heat days in areas with a larger share of <5 year olds but not in areas with larger shares of >65 year olds, whereas we find the opposite for freezing days. Importantly, for our main research question - how aggregate fiscal burdens may be affected by warming and the associated macroeconomic consequences - we observe comparable average marginal effects of heat days here as in the benchmark. Given that one of the estimates (Column 3) is attenuated, however, the modeling analysis also shows results that set all heat-healthcare cost impacts to zero as a lower bound on the overall effects.

A1.2 Plausibility and Fee-for-Service Analysis

The empirical results suggest that annual public health expenditures increase by around 0.15% per additional extreme heat day on average in current climatic conditions. While our BEA data do not allow for a detailed delineation of the underlying mechanisms, prior micro evidence from hospital data has associated extreme heat days with increases in a wide range of adverse health outcomes such as accidental injuries, cardiovascular, metabolic, and infectious diseases, and mental illness (Gould et al. 2025; Rizmie et al. 2022; Mullins and White 2019; Karlsson and Ziebarth 2018). Qualitatively, an increase in aggregate healthcare expenditures is thus expected.

Quantitatively, we gauge the plausibility of our estimates as follows. At the annual(ized) level, prior micro studies using daily hospital data find effects that are smaller but of similar order of magnitude. For example, Karlsson and Ziebarth (2018) estimate a +0.05% annual increase in hospital admissions per +1 day with maximum temperatures above 30°C in Germany, whereas Gould et al.'s (2025) estimates imply a +0.03% increase in annual emergency department visits per +1 day with average temperatures above 34°C in California. We consider two possible explanations for our higher magnitude estimate. The first possibility is that extreme heat leads to larger increases in *non-hospital* healthcare utilization that are captured by our data but not by prior hospital-based studies. While we cannot test this hypothesis in the BEA data, below we provide suggestive evidence from Medicare Fee-for-Service (FFS) utilization records that other medical services may indeed be more responsive to extreme heat than hospital admissions, such as *home*

Table A4: Robustness: Age Interactions

Dep. Var.:	ln(Public Medical Expenditures/Pop.)			
	(1)	(2)	(3)	(4)
Extreme Heat Days$_{j,t}$	0.00378	0.00351	-0.00193	-0.00267**
	(0.00302)	(0.00379)	(0.00348)	(0.00122)
Extreme Heat Days$_{j,t}$ $\times$ $\overline{T}_{m,j}$	-0.00038***	-0.00037**	-0.00003***	-0.00000
	(0.00013)	(0.00015)	(0.00001)	(0.00000)
Extreme Heat Days$_{j,t}$ $\times$(%<5)	0.06923*	0.07018*	0.05551	0.03513**
	(0.03691)	(0.03694)	(0.03797)	(0.01441)
Extreme Heat Days$_{j,t}$ $\times$ (%>65)	-0.00784	-0.00759	-0.00878	0.00414
	(0.01301)	(0.01337)	(0.01308)	(0.00356)
Pop-weighted Avg. (MFX$_{\text{Extreme Heat}}$)	0.0019	0.0019	0.0005	0.0001
Freezing Days$_{j,t}$	0.00004	-0.00012	0.00007	0.00021
	(0.00089)	(0.00089)	(0.00081)	(0.00085)
Freezing Days$_{j,t}$ $\times\overline{T}_{m,j}$	0.00001	0.00000	0.00000*	0.00000
	(0.00002)	(0.00002)	(0.00000)	(0.00000)
Freezing Days$_{j,t}$ $\times$ (%<5)	-0.01563**	-0.01473*	-0.01682**	-0.01678*
	(0.00785)	(0.00786)	(0.00791)	(0.00867)
Freezing Days$_{j,t}$ $\times$ (%>65)	0.00620**	0.00606**	0.00585*	0.00656**
	(0.00306)	(0.00307)	(0.00306)	(0.00286)
Pop-weighted Avg. (MFX$_{\text{Freezing}}$)	0.00001	-0.00002	-0.0001	0.00002
Obs.	70,239	70,239	70,239	70,239
Adj. R-Sq.	0.971	0.971	0.971	0.971
#Counties (Clusters)	3,055	3,055	3,055	3,055
"Heat" Measure	Avg.>32C	Avg.>32C	Avg.>32C	Max.>35C
"Freezing" Measure	Avg.<0C	Avg.<0C	Avg.<0C	Min.<0C
$\overline{T}_{m,j}$ is average of:	Temp.	Temp.	#Heat/Freeze Days	#Heat/Freeze Days

Table shows results of linear regression of log of county-year public medical expenditures per capita (1996-2019, from BEA) on the number of "heat" days (defined as avg. daily temperature>32C in Cols 1-3 and max. daily temperature>35C in Col. 4), "freezing" days (defined as avg. daily temperature<0C in Cols 1-3 and min. daily temperature<0C in Col. 4) both in levels and interacted with climate measures $\overline{T}_{m,j}$ (avg. temperature in Cols. 1-2 and avg. number hot/cold days in Cols. 3-4) (based on data from PRISM) and the share of the population under 5 and above 65, along with county fixed effects, linear state-level trends, year fixed effects and controls for log of county populations, prior to current year population growth, percent non-hispanic whites (all demographics from the National Center for Health Statistics), log and growth of real per capita income (from BEA), precipitation (2nd order poly-nominal) plus interaction of precipitation and "heat"/"freezing" days in Col. 2 (based on data from PRISM), and the number of hurricane days in the county-year (NOAA Storm Events Database). Regressions are weighted by county populations. Standard errors are heteroskedasticity-robust and clustered at the county level. P-values are labeled: *** p<0.01, ** p<0.05, * p<0.1

healthcare. The second possibility is of course bias or spurious inference. In recognition of this possibility, Section 5 shows quantitative model results both with and without heat healthcare cost impacts. The central finding of this paper - that climate change may impose significant fiscal burdens and thereby increase the social cost of carbon for the U.S. economy - is robust to this modeling variant.

Our supplemental data analysis proceeds as follows. We obtain "Market Saturation and Utilization Data" from the Centers for Medicare & Medicaid Services (CMS). These data provide, at the county of residence-year level, utilization rates for 19 different types of medical services. To the best of our knowledge these are the only publicly accessible U.S. national-scale county-year data providing such disaggregated healthcare utilization information. We aggregate similar services into 14 categories for parsimony.[2,3] The data are only available from 2015-2024 and come with additional limitations. First and most importantly, the data only cover Medicare FFS claims, and thus exclude other public health programs covering a broader segment of the population. Given our and prior literature's findings on the importance of, e.g., young children in the healthcare utilization response to extreme heat, this is an important limitation. Even among (mainly elderly) Medicare beneficiaries there is also significant variation both across time and space in the fraction choosing FFS vs. Medicare Advantage. On the one hand, the analysis conditions on the number of FFS beneficiaries in the county-year (formally via an offset) to isolate the effects of temperatures on utilization *rates.* On the other hand, however, the analysis is not representative of the U.S. (public healthcare recipient) population. Inference is further complicated by the fact that changes in the number of FFS beneficiaries in each county vary differentially with climatic conditions.[4] A final limitation is that the list of medical services covered is not exhaustive as the data's purpose is to help providers understand demand for key services in different locations. The analysis is thus suggestive. We estimate the effects of temperature extremes on healthcare utilization rates via pseudo-Poisson maximum likelihood (Correia et al. 2020) with temperature and climate measures from the benchmark specification, along with state-specific trends and year fixed effects.

The results suggest the possibility of larger increases in demand for certain non-hospital healthcare services, such as home healthcare, laboratory services, and telemedicine. In terms of economic significance, laboratory and home health are the first and third largest expenditure categories in

[2] We aggregate different laboratory services into one "Laboratory" category, combine chiropractor and podiatry services with physical and occupational health into "Therapy+", and combine endocrinology, neurology, pulmonology, and ophthalmology into "Specialty" services.

[3] From a multiple hypothesis testing perspective one should be cautious about results from simultaneously considering 14 different outcomes. Given the suggestive nature of the analysis, we do not adjust standard errors, but note this as an additional caveat.

[4] For example, the correlation between the percent change in the number of FFS beneficiaries from 2015 to 2024 for each county with (i) average long-run temperature is -0.32, whereas for (ii) the number of days with average temperatures above 32°C it is only -0.01. This difference is not surprising given the high uptake of Medicare Advantage in some southern states that feature high average temperatures but few extreme heat days, such as Georgia and Alabama.

the sample, respectively, averaging total expenditures of $48 billion and $16 billion per year. Interestingly, the results also imply significant decreases in cardiac rehabilitation care as a result of hot days in cold counties but increases from hot days in sufficiently warm counties. We conjecture that this pattern is driven by differential cardiac mortality effects which leave fewer respectively more survivors in cardiac rehabilitation care. Given that the "number of beneficiaries" term used to calculate utilization rates includes anyone who was a beneficiary for at least one month during the year it would also include individuals who perished during the year. Before proceeding, we note that the results of these Medicare FFS utilization rates are more sensitive to specification than the benchmark analysis. Again, this is not surprising given the selected nature of the data and differential correlations of FFS beneficiaries with competing climatic indicators. With these caveats in mind, the analysis does suggest the possibility that demand for certain non-hospital medical services may be more responsive to extreme heat.

	(1)	(2)	(3)	(4)	(5)	(6)	(7)
Utilization Rate:	Ambulance	Cardiac Rehab	Dialysis	Federally	Home Health	Hospice	Laboratory
Avg.T.>32C Days$_{j,t}$	0.0011	-0.0277***	-0.0007	0.0168*	0.0141***	-0.0030	0.0074***
	(0.0022)	(0.0059)	(0.0035)	(0.0092)	(0.0037)	(0.0021)	(0.0022)
Avg.T.>32C Days$_{j,t} \times \overline{T}_{m,j}$	-0.0001	0.0014***	-0.0000	-0.0008*	-0.0007***	0.0001	-0.0004***
	(0.0001)	(0.0003)	(0.0002)	(0.0004)	(0.0002)	(0.0001)	(0.0001)
Avg. MFX$_{\text{Heat}}$	-0.0000	-0.0100***	-0.000839	0.00642*	0.00539***	-0.00104	0.00281**
Avg.T.<0C Days$_{j,t}$	0.0010***	-0.0011*	-0.0004	-0.0027***	0.0013***	0.0009***	0.0002
	(0.0003)	(0.0006)	(0.0004)	(0.0010)	(0.0003)	(0.0003)	(0.0004)
Avg.T.<0C Days$_{j,t} \times \overline{T}_{m,j}$	-0.0001**	0.0001	-0.0000	0.0003***	-0.0001***	-0.0000*	-0.0000
	(0.0000)	(0.0001)	(0.0000)	(0.0001)	(0.0000)	(0.0000)	(0.0000)
Avg. MFX$_{\text{Cold}}$	7.70e-05	-0.000387	-0.000499	0.000957	-0.000226	0.000317	-3.34e-05
Obs.	31,012	25,822	25,972	28,432	30,442	29,952	31,056
Pseudo R2	0.995	0.929	0.977	0.974	0.995	0.985	0.997
#Clusters (Counties)	3102	2583	2598	2844	3045	2996	3107

Table shows PPML estimates of how temperature extremes affect Medicare FFS utilization rates of each indicated service category (column). Dependent variable is the number of users of the service in the county-year (from CMS MSUD data) with an offset for ln(number of eligible beneficiaries) in the county-year (2015-2024). Control variables include temperature-day counts both in levels and interacted with county average temperature, county and year fixed effects, and state trends. Standard errors robust and clustered at the county level. *** $p<0.01$, ** $p<0.05$, * $p<0.1$

	(8)	(9)	(10)	(11)	(12)	(13)	(14)
Utilization Rate:	Care Hospital	Occupational	Preventive	Psycho	Skilled	Specialty	Telemed
Avg.T.>32C $\text{Days}_{j,t}$	0.0080	0.0184***	0.0038*	0.0029	0.0019	0.0030	0.0406***
	(0.0182)	(0.0047)	(0.0022)	(0.0044)	(0.0040)	(0.0057)	(0.0115)
Avg.T.>32C $\text{Days}_{j,t} \times \overline{T}_{m,j}$	-0.0005	-0.0008***	-0.0002*	-0.0001	-0.0001	-0.0001	-0.0019***
	(0.0009)	(0.0002)	(0.0001)	(0.0002)	(0.0002)	(0.0003)	(0.0006)
Avg. MFX_{Heat}	0.00153	0.00756***	0.00134	0.00108	0.000143	0.00167	0.0166***
Avg.T.<0C $\text{Days}_{j,t}$	0.0007	0.0011***	0.0007***	0.0022***	0.0014***	0.0003	-0.0064***
	(0.0018)	(0.0004)	(0.0002)	(0.0003)	(0.0004)	(0.0006)	(0.0013)
Avg.T.<0C $\text{Days}_{j,t} \times \overline{T}_{m,j}$	0.0000	-0.0001**	-0.0000***	-0.0002***	-0.0001**	-0.0000	0.0003***
	(0.0002)	(0.0000)	(0.0000)	(0.0000)	(0.0000)	(0.0001)	(0.0001)
Avg. MFX_{Cold}	0.000913	-4.82e-05	0.000197	-0.000131	0.000449	-0.000118	-0.00215
Obs.	15,422	30,742	31,052	30,362	30,392	28,382	24,584
Pseudo R2	0.921	0.995	0.999	0.994	0.991	0.980	0.966
#Clusters (Counties)	1543	3075	3106	3037	3040	2839	3074

Table shows PPML estimates of how temperature extremes affect Medicare FFS utilization rates of each indicated service category (column). Dependent variable is the number of users of the service in the county-year (from CMS MSUD data) with an offset for ln(number of eligible beneficiaries) in the county-year (2015-2024). Control variables include temperature-day counts both in levels and interacted with county average temperature, county and year fixed effects, and state trends. Standard errors robust and clustered at the county level. *** $p<0.01$, ** $p<0.05$, * $p<0.1$

Table A5: Medicare Fee-for-Service Analysis

A1.3 Healthcare Cost Effect Dynamics

One may wonder whether the observed expenses simply move forward expenses that would have otherwise occurred at later points in time. While this kind of "harvesting" is well-documented for *mortality* effects of heat (at a high frequency level), for healthcare utilization we note three points. First, the dynamics are potentially different: For California emergency department (ED) visits, White (2017) documents that the effects of a hot day actually *increase* after the hot day itself, with an estimated cumulative 31-day effect that is 45% larger than the contemporaneous impact. This finding is consistent with other studies documenting lagged hot day increases to accidents (Drescher and Janzen 2025) and productivity (Somanathan et al. 2021) which may be due to, e.g., sleep disruptions. One must caution that this result is not universal: Karlsson and Ziebarth

(2018) find substantially smaller effects of hot days on hospital admissions at the monthly vs. daily level. Second, however, even in this setting there is no evidence of harvesting past 1 month. That is, Karlsson and Ziebarth (2018) find similar sized effects when aggregating to the monthly vs. annual data. This paper's annual focus should thus be robust to shorter term harvesting effects. Finally, we empirically confirm the absence of harvesting in our analysis by adding lagged temperatures to the benchmark specification. Harvesting would imply a *negative* coefficient on the lagged number of hot days. However, Table A6 shows that, if anything, lagged effects may be positive, suggesting that our benchmark specification may underestimate longer-term effects of heat days.

Dep. Var.:	ln(Public Medical Expenditures/Pop.)				
	(1)	(2)	(3)	(4)	(5)
Extreme Heat Days$_{j,t}$	0.00359***	0.00448**	0.00127***	0.00006	0.00015
	(0.00112)	(0.00183)	(0.00017)	(0.00011)	(0.00009)
Extreme Heat Days$_{j,t}$ $\times$ $\overline{T}_{m,j}$	-0.00014**	-0.00017**	-0.00002***	0.00000	
	(0.00006)	(0.00009)	(0.00001)	(0.00000)	
Extreme Heat Days$_{j,t-1}$	0.00146	0.00418**	0.00007	-0.00001	0.00038***
	(0.00150)	(0.00197)	(0.00019)	(0.00009)	(0.00010)
Extreme Heat Days$_{j,t-1}$ $\times$ $\overline{T}_{m,j}$	-0.00005	-0.00016*	0.00002***	-0.00000	
	(0.00008)	(0.00009)	(0.00000)	(0.00000)	
Obs.	70,239	70,239	70,239	70,239	70,239
Adj. R-Sq.	0.972	0.972	0.972	0.972	0.972
#Counties (Clusters)	3,055	3,055	3,055	3,055	3,055
"Heat" Measure	Avg.>32C	Avg.>32C	Avg.>32C	Max.>35C	Avg.>97.5th Pct.
"Freezing" Measure	Avg.<0C	Avg.<0C	Avg.<0C	Min.<0C	Avg.<2.5th Pct.
$\overline{T}_{m,j}$ is average of:	Temp.	Temp.	#H/F Days	#H/F Days	-

Table shows benchmark specifications (see Table 1) with the addition of the 1-year lagged value of all weather variables (heat days, freezing days, and their interactions with average climate, precip., precip^2, hurricane days, and in Col. (2) heat and freezing days interacted with preciptation. P-values: *** p<0.01, ** p<0.05, * p<0.1

Table A6: Lagged Temperature Effects

A1.4 Future Temperature Projections

To illustrate the downscaled daily temperature data underlying the climate impact projections, Figure A5 showcases the average projected change in the number of days with average temperatures above 32°C for each county, calculated from Gergel et al.'s (2024) downscaled and bias-corrected temperature projections across 17 climate models in CMIP6 which we combine with 2020 U.S. Census block population data to compute population-weighted county-level averages.[5] The figure specifically illustrates the difference in the average annual number of extreme heat days in mid-century (2055-64) compared to the current period (2025-34) in the SSP3-7.0 scenario, which is associated with a CMIP6 ensemble mean warming projection of +3.16°C by the end of the 21st Century over a 1995-2014 baseline (Tebaldi et al. 2021). The projections indicate large potential increases in hot days, with up to 45 *additional* extreme heat days per year in some locations. By the end of the century, the corresponding figure would be up to 95 additional hot days per year, although we stress that the model endogenizes global temperatures and thus does not follow a given temperature scenario such as SSP3-7.0.

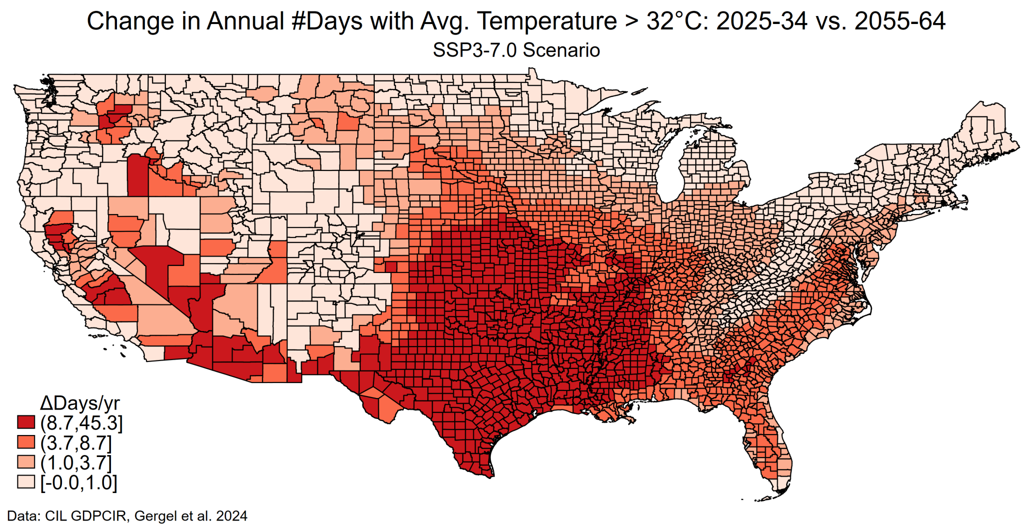

Figure A5: Projected change in the average number of days per year where average temperatures exceed $32°C$ between the 2025-34 period and 2055-64 in the SSP3-7.0 scenario across 17 climate models participating in CMIP6 and which are included in downscaled temperature projections of Gergel et al. (2024). Temperature exceedance counts at the grid cell level are population-weighted based on 2020 U.S. Census block population data and aggregated to the county level.

A1.5 Heat Healthcare Cost Damage Function Robustness

Our benchmark approach fits a weighted quadratic damage function to the heat-day healthcare cost projections. That is, we pool projected mean (across Monte Carlo runs within a warming

[5] Temperature exceedances are first calculated at the grid-cell level before aggregating up to the county-level with population weights.

scenario i) aggregate U.S. healthcare cost increases from extreme heat days in each year, y_{it}, link them to the relevant global mean surface temperature change implied by the MAGICC model (Meinshausen et al. 2011), and fit the data to a quadratic in temperature: $y_{it} = \beta_1(TC_{it})^2+\epsilon_{it}$. We weigh observations from the more recent CMIP6 model ensemble (SSP2-4.5 and SSP3-7.0) at *twice* the weight of the older CMIP5 RCP 8.5 projections, but retain the latter due to their advantage of having a probabilistic interpretation thanks to the addition of surrogate models ("SMME", Rasmussen et al. 2016). As shown in the main paper Appendix, the benchmark coefficient is similar upon inclusion of an intercept.

In order to evaluate the robustness of our results to the quadratic form, we repeat this estimation procedure for both a cubic ($y_{it} = \beta_1(TC_{it})^2 + \beta_2(TC_{it})^3 + \epsilon_{it}$) and quartic polynomial ($y_{it} = \beta_1(TC_{it})^2 + \beta_2(TC_{it})^3 + \beta_3(TC_{it})^4 + \epsilon_{it}$). Figure A6 shows the corresponding best-fit lines. While the implied damage functions differ at extreme levels of warming, for the most empirically relevant range of expected global temperature change (<$4°C$), they are similar.

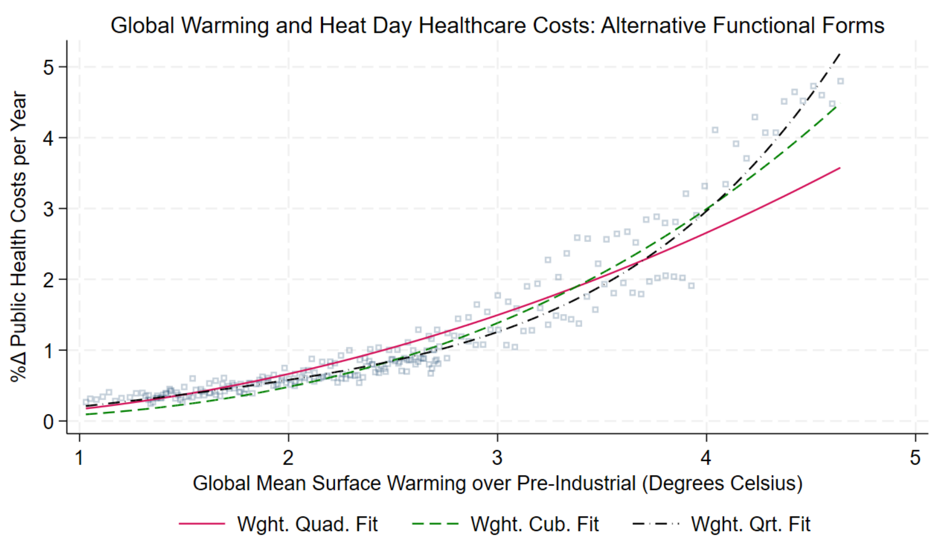

Figure A6: Robustness of heat healthcare damage function to functional form

A1.6 Freezing Day Impacts and Alternative Adaptation Formulation

The benchmark heat cost estimation adopts Table 1 Column 1 as preferred specification and focuses on precisely estimated heat day impacts. Here we show results using Column 3 results instead, which differ by proxying adaptation based on the average number of extreme heat and cold days in the county over the past 30 years, and yield precisely estimated freezing day impacts in addition to hot day effects.

Figure A7 shows the results, which are extremely similar to the benchmark: The average of projected end-of-century healthcare cost increase is +1.7% with Col. 3 and +1.9% with Col. 1. This similarity may be initially surprising as the present day marginal cost impacts of heat days are on average lower with the Column 3 specification. However, an important difference in future projections is that adaptation can advance more quickly with Column 1's specification. This is because the moving average of county temperature can increase under a wider set of conditions than the moving average count of extreme heat days. For example, if a county experiences a summer with an unusually high number of 30°C average temperature days, this would increase next year's moving average of county temperature but not its 30-year moving average count of 32°C plus days. For this reason we also prefer long-run average temperature as a more comprehensive measure of heat risk than the average number of 32°C+ days.

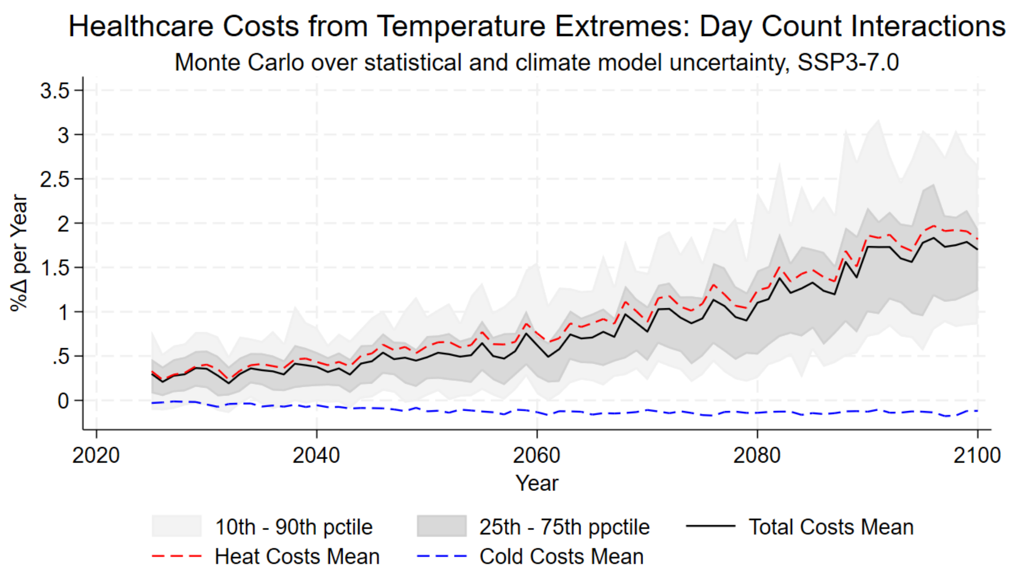

Figure A7: Healthcare cost projections using Table 1 Column 3 results

A2 Fiscal Impact Background Considerations

A2.1 Sectoral Coverage in Prior Damage Functions

This paper argues that changes in the costs of providing public services constitute an important and new source of climate change impacts on the U.S. economy. Naturally one may be concerned about double-counting and the extent to which the costs quantified in the analysis are already covered by prior damage functions. Table A7 summarizes key components of the main motivating U.S. damage functions used in the analysis and prominent other examples from the literature. On the one hand, there is a benchmark set of impact channels included in all studies: agriculture, energy costs, sea-level rise (SLR),[6] and mortality effects which are typically valued through the value of statistical life (VSL). Importantly, however, the other costs that are the focus of our analysis - public healthcare, wildfires, public infrastructure, and public aid - are generally missing in standard damage functions.

Two important nuances are worth noting. First, one may wonder about the extent to which prevailing adaptation cost estimates may already account for healthcare expenditures. As shown in Table A7, however, adaptation costs to mitigate climate health impacts are excluded in most benchmark models. The WITCH model considers some (reactive) adaptation costs in health based on Tol and Dowlatabadi (2001), but these appear to be set to zero for the United States, presumably due to their focus on vector-borne diseases.[7] The Climate Impacts Lab (CIL) approach based on Carleton et al. (2022) quantifies adaptation costs indirectly by assuming that observed differences in excess mortality from hot daily temperatures in warmer climates – marginal adaptation benefits - equal marginal adaptation costs if agents in each location are optimizing. These costs are again monetized from their estimated units - mortality rate changes - into dollars based on the VSL approach. The extent to which public health expenditures are affected by climate change thus remains an open question. Our quantification of the difference in the SCC with vs. without fiscal costs also focuses on the RICE and SEAGLAS U.S.-specific damage functions which omit health adaptation costs. Second, Hsiang et al. (2017) includes property hurricane damages based on the RMS North Atlantic Hurricane Model. This is a proprietary model used by the insurance industry to model property exposure. It considers neither public transfer payments nor public infrastructure adaptation costs.

Section 5 Figure 5 shows that the main result of our study - namely that fiscal costs of climate change have first-order welfare and policy implications - broadly survives additional exclusions from the fiscal damage function. For example, excluding not only hurricane aid but also crop insurance subsidy and all other government consumption impacts leads to a smaller but still first-order effect of the remaining fiscal costs on welfare and the SCC.

[6] With regards to double-counting risk for sea-level rise, we note that while sea-level rise impacts are considered in Hsiang et al. (2017) they feature limited representation in their estimated damage function we use due to limited mapping into temperature change.

[7] See Table 8.3 in WITCH documentation ([https://doc.witchmodel.org/], last accessed August 2025).

Sector	**RICE Nordhaus (2010)**	**SEAGLAS Hsiang et al. (2017)**	FUND Anthoff and Tol (2014)	GIVE Rennert et al. (2022)	WITCH Emmerling et al. (2016)	CIL-EPA (2022)
Agriculture	✓	✓	✓	✓	✓	✓
Energy	✓	✓	✓	✓	✓	✓
SLR	✓	✓	✓	✓	✓	✓
Mortality (VSL)	✓	✓	✓	✓	✓	✓
Mortality adaptation costs	**X**	**X**	X	X	(✓)	✓
Labor	**X**	✓	X	X	(✓)	✓
Healthcare	**X**	**X**	X	X	X	X
Wildfires	**X**	**X**	X	X	X	X
Hurricanes	**X**	(✓)	(✓)	X	X	X
Public Infrastructure	**X**	**X**	X	X	X	X
Public transfers	**X**	**X**	X	X	X	X

Table A7: Table summarizes sectoral coverage in prior climate damage functions. RICE and SEAGLAS are used in the present model; others are included for reference. (✓) indicates partial coverage (see text). Sectoral listings are not exhaustive as models may include additional sectors (e.g., crime in SEAGLAS, forestry in FUND, etc.).

A2.2 Mortality and Social Security

One of the channels through which climate change could affect public budgets is via mortality impacts on participation in programs such as Social Security. Since elderly populations are well-known to be disproportionately vulnerable to ambient temperatures (e.g., Carleton et al. 2022), and since early estimates suggested that warming may lead to significant increases in (elderly) mortality rates (e.g., Deschenes and Greenstone 2011; Hsiang et al. 2017), one might thus be concerned that our analysis overestimates net fiscal impacts by disregarding potential cost savings from decreased Social Security participation. In order to gauge the potential magnitudes of these effects, we first consider recent literature on the U.S. (elderly) mortality impacts from warming.[8,9] As shown in Table A8, more recent studies actually project *declines* in elderly mortality due to

[8] We focus on studies using broad-scale data and modern econometric techniques but note that similar patterns can be found in other studies. For example, using data from 106 U.S. cities, Lee and Dessler (2023) estimate that warming leads to reductions in temperature mortality when adaptation is considered.

[9] We focus on the literature using mortality data instead of considering Social Security empirically in our own analysis as the main margin of interest - changes in participation due to mortality - cannot be as well isolated with our local expenditure data due to confounders such as migration. (We note that this is not a direct concern for our main analysis of healthcare spending impacts *per capita*).

climate change in the United States. Heutel et al. (2021) argue that this is at least in part due to the development of new econometric techniques that allow for heterogeneous marginal effects of ambient temperatures and use those estimates to also consider future adaptation to warming (as is done in our analysis of healthcare expenditure impacts of warming). Heutel et al.'s analysis shows that, using the same data, those two methodological innovations change the projected warming impacts from an increase to a decrease in elderly mortality.

Study	RCP	Time	Population: All	Population: 65+	Het. Marg. Effects?	Future Adaptation?
Gould et al. (2025)	4.5	2050	-0.43%	Largest mortality	x	x
	4.5	2100	-0.77%	decline (Fig S12)	x	x
Carleton et al. (2022)	8.5	2100		-0.2 deaths/100k	✓	✓
	4.5	2100		-12.7 deaths/100k	✓	✓
Heutel et al. (2021)	8.5	2080-99		-0.53%	✓	✓
	4.5	2080-99		-0.06%	✓	✓
	8.5	2080-99		+0.76%	x	x
	4.5	2080-99		+0.18%	x	x
Hsiang et al. (2017)	per $^{\circ}C$	2080-99	+5.4 deaths/100k		x	x
Deschenes and Greenstone (2011)	A1F1	2070-99	+3%	+3%	x	x

Table A8: Literature estimates of climate change impacts on US mortality (via ambient temperature changes). "RCP" (Representative Concentration Pathways) refers to warming scenarios where RCP 4.5 (8.5) is a moderate (very high) warming scenario. "A1F1" also refers to a high warming scenario. "Het. Marg. Effects" indicates whether a projection uses temperature-mortality estimates that incorporate heterogeneity in marginal effects as a function of local characteristics. "Future Adaptation" indicates whether projections incorporate changes in marginal effects of ambient temperatures as each location warms. Carleton et al. (2022) figures correspond to mortality-only effects (excluding adaptation costs but accounting for adaptation effects on mortality changes) from Tables II and F.2.

It is nonetheless instructive to also consider what the order of magnitude of cost savings implied by the older estimates would be. Deschenes and Greenstone's (2011) estimates - which are also used by Hsiang et al. (2017) - imply that high warming would result in the loss of around 418k life-years per year among the 65+ population. In today's economy, Social Security expenditures for Old Age and Survivors Insurance average around \$21.1k per year (\$2022)[10]. Imposing future warming and elderly populations on today's economy would thus imply an upper bound of 418k*\$21.1k = \$8.8 billion in annual cost savings, an order of magnitude less than our benchmark estimate of current annual fiscal climate costs (\$88 billion per year in 2026).

[10] Calculated based on current monthly benefits (\$1,918 in July 2025, \$2025) times twelve and converted to \$2022 based on the US Consumer Price Index. Data source URL (accessed August 2025): [https://www.ssa.gov/policy/docs/quickfacts/stat_snapshot/]

A2.3 Insurance Market Support

Both public and private property insurance markets are struggling to cope with rising climatic risks in many parts of the United States (e.g., Boomhower et al. 2024). Instability in insurance markets - such as from rapidly rising rates, declining availability, or catastrophic losses - can create a need for public support for insurance markets to protect property values and financial markets. A core challenge to quantifying this exposure, however, is that many government-run insurance support programs currently legally stipulate that costs *should* be paid by insurance ratepayers and not taxpayers.[11] For example, the California FAIR plan - a property insurer of last resort - exists due to state law but is funded by participating insurers. Even the funding shortfalls in the aftermath of the catastrophic 2025 Los Angeles wildfires were met through a $1 billion assessment on participating insurers (CDI 2025). Another prominent example is the Florida Hurricane Catastrophe Fund which effectively provides partial reinsurance to residential property insurers. Again, though publicly organized, this fund is financed from reimbursement premiums from insurers operating in the state, along with investment income from the fund. If needed after a hurricane, the fund may also issue bonds, although the statutes specify that "The funds, credit, property, or taxing power of the state or political subdivisions of the state shall not be pledged for the payment of such bonds."[12] The Texas Wind Insurance Association (TWIA), also an insurer of last resort for wind and hail risks, operates similarly, with its website clarifying that "TWIA is not a state agency and does not receive General Revenue funds or any other state funds for operations."[13] Importantly, however, the need for government to provide assistance in certain situations is becoming increasingly apparent. For example, the National Flood Insurance Program (NFIP) has accumulated tens of billions of dollars of debt at the U.S. Treasury over the past 20 years in part due to its failure to charge actuarially fair rates against a backdrop of rising climatic risks. While NFIP is supposed to repay both its debt and the associated interest from premium revenues and other inflows, in 2017 $16 billion in debt were cancelled by the U.S. Treasury after a series of highly destructive hurricane events (CRS 2025). Given the ad hoc nature of these outlays, however, and given our model's focus on current law as baseline for future projections, we omit this impact channel from the quantitative estimation.[14] Nonetheless, given the economic

[11] Explicitly taxpayer funded property insurance support funds do exist but are typically modest in size. For example, Louisiana's "Insure Louisiana Incentive Program" was created with a $45 million budget allocation (LA HB1 2023 1st Special Session). Florida's "Reinsurance to Assist Policyholders" program is currently capped at $900 million (Florida House Bill 5013, July 2025).

[12] Florida Statutes Paragraph 215.555, URL (accessed August 2025): https://www.leg.state.fl.us/Statutes/index.cfm?App_mo 0299/0215/Sections/0215.555.html

[13] See TWIA website, URL (accessed August 2025): [https://www.twia.org/about-us/funding-101/]

[14] For NFIP, current law also forsees a new pricing approach ("Risk Rating 2.0") wherein insurance premiums are based more closely on individual properties' flood risks, which could limit fiscal shortfalls from rising flood risks going forward.

significance of property markets, one should bear in mind that the need for more public financial support may well constitute an economically significant fiscal cost of climate change in the future.

A2.4 Further Details on Fiscal Impact Estimates

This section provides further information on government study-based estimates of fiscal costs that are used to calibrate our damage function, specifically with regards to whether and how they account for adaptation to future warming and uncertainty.

First, CBO's (2016) estimates of changes in hurricane-related federal expenditures consider two potential shifters of vulnerability to a storm conditional on climatic conditions (which include sea levels, hurricane frequency, and intensity): Population and per capita income growth. For both of these co-variates, CBO considers mixed effects on hurricane vulnerability. For population growth, these include an increase in the population at risk (+) but also protection from wind damages from denser housing developments (-). For per capita income growth, these include an increase in the value of the housing stock at risk (+) but also a decrease from investment in adaptation and infrastructure upgrades (-). On net, CBO adopts positive but less-than-proportional effects of both coastal population and income growth on the dollar value of damages, ceteris paribus. The broader literature has repeatedly identified the US as an outlier in its hurricane vulnerability (e.g., Hsiang and Narita 2012; Bakkensen and Barrage 2025) including with regards to the fact that, unlike other countries, there is no evidence of adaptation with growing income levels (Bakkensen and Mendelsohn 2016). With regards to uncertainty, CBO conducts extensive Monte Carlo analysis consider uncertainty over both climatic projections (hurricanes, sea level rise) and over the economic impacts. Among other inputs, they use downscaled CMIP5-based projections of changes in hurricane activity from both Emanuel (2013 and Knutson et al. (2013) and probabilistic sea level rise projections from Kopp et al. (2014). The estimates we use represent the mean from these simulations and therefore account for the right tail of the future damage distribution.

Second, the Forest Service's (FS, 2016) analysis of fire suppression cost changes on FS and Department of Interior (DOI) lands adopts a two-stage empirical approach: First, they estimate how area burned is affected by temperatures (average of daily maximum over the fiscal year), and second, they estimate how fire suppression expenditures vary with area burned to construct an overall damage function. For all but the second step with DOI data, they use fixed effects panel regressions with controls for structural changes in fire management in 2000 and 2011, respectively. With regards to further vulnerability co-variates, FS tested the inclusion of both population and household income levels, but opted not to include them in the preferred specification based on model fit considerations. For uncertainty, the analysis conducts a Monte Carlo analysis considering estimation uncertainty and climate projection uncertainty over downscaled output from the climate models considered (three models from CMIP5). Headline figures refer to the median across these simulations.

Third, the EPA's (2017) estimates of both changes in urban drainage infrastructure and road maintenance costs with warming explicitly model adaptation. For roads, the estimates are based on the combination of an engineering model, U.S. road data, and downscaled climate model projections (for temperature, precipitation, and freeze-thaw cycles from 5 GCMs for RCP 4.5 and 8.5). The analysis considers both "reactive adaptation" in the form of additional maintenance required to maintain current service without structural changes to roads, and "proactive adaptation" measures (e.g., "change asphalt mix to include binder with appropriate temperature performance") both in terms of their costs and benefits (i.e., reactive maintenance costs avoided). The estimates we use are 5-GCM mean. In terms of adaptation scenarios, we adopt a middle ground (average) between the two extremes of no proactive adaptation and 100% optimized upgrades to the U.S. road network. For urban drainage, the estimates specifically represent adaptation costs required to maintain current service. The estimates are based on the EPA's Storm Water Management Model with climate change, again with some consideration of uncertainty across 5 climate models and two warming scenarios.

While most of the incorporated estimates thus consider adaptation and uncertainty, OMB's (2016) estimates of healthcare costs from air quality changes under a warming climate from Garcia-Menendez (2015) are based on a more limited set of physical modeling and impact mappings. The latter uses dose-response mappings from the U.S. EPA's regulatory impact assessments in the present. This component of the damage function is very small and moreover almost certainly an underestimate of air quality impacts as it abstracts from changes in wildfire smoke. The quantitative analysis nonetheless presents results also for a scenario that disregards all public expenditure impacts except for our empirically measured temperature and hurricane effects.

A3 Theoretical Derivations

It is straightforward to show (following an analogous derivation to the one in Barrage, 2020) that the primal social planner's problem is as follows:

$$
\begin{aligned}
&\max \sum_{t=0}^{\infty} \beta^t [\underbrace{[U(C_t, L_t; T_t, f^u(G_t^c, \gamma_t^u)) + \phi \left[U_{ct}C_t + U_{lt}L_t - U_{ct}G_t^T(T_t)\right]]}_{\equiv W_t} \\
&+ \sum_{t=0}^{\infty} \beta^t \lambda_{1t} \left[\begin{array}{c} Y_t(A_{1t}, K_{1t}, L_{1t}, E_t; T_t, f^y(G_t^c, \gamma_t^y)) + (1-\delta(SLR_t, \Lambda_t^{slr}))K_t \\ -C_t - K_{t+1} - \gamma_t^c(G_t^c, T_t) - \gamma_t^y - \gamma_t^u - \gamma_t^{slr} - \Theta_t(\mu_t)E_t \end{array} \right] \\
&+ \sum_{t=0}^{\infty} \beta^t \xi_t [T_t - F_t \left(\mathbf{S}_0, (1-\mu_0)E_0 + E_0^{ROW}, ..., (1-\mu_t)E_t + E_t^{ROW}, \boldsymbol{\eta}_0, ...\boldsymbol{\eta}_t\right)] \\
&+ \sum_{t=0}^{\infty} \beta^t \lambda_{lt} \left[L_t - L_{1t} - L_{2t}\right] + \sum_{t=0}^{\infty} \beta^t \lambda_{kt} \left[K_t - K_{1t} - K_{2t}\right] \\
&+ \sum_{t=0}^{\infty} \beta^t \zeta_t [SLR_t - f_t^{slr}(T_0, T_1, ...T_t)] + \sum_{t=0}^{\infty} \beta^t \omega_t \left[F_2(A_{Et}, K_{2t}, L_{2t}) - E_t\right] \\
&+ \sum_{t=0}^{\infty} \beta^t \eta_{St} \left[f^{slr}(\Gamma_t) - \Lambda_t^{SLR}\right] + \sum_{t=0}^{\infty} \beta^t \eta_{\Gamma t} [\Gamma_t(1-\delta^\Gamma) + \lambda_t^{slr} - \Gamma_{t+1}] \\
&- \phi \left\{U_{c0} \left[K_0 \left\{1 + (F_{1k0} - \delta)(1 - \overline{\tau_{k0}})\right\} + B_0\right]\right\}
\end{aligned}
$$

We note that we have substituted in the feasibility constraints for public adaptation $\Lambda_t^u = f^u(G_t^c, \gamma_t^u)$ and $\Lambda_t^y = f^y(G_t^c, \gamma_t^y)$.The derivations below utilize the assumption of separability in preferences over temperature. Notationally, we denote partial derivatives with a mix of subscripts (e.g., $Y_{K1t} = \frac{\delta Y_t}{\delta K_{1t}}$) and standard notation (e.g., $\frac{\partial Y_t}{\partial T_t}$) to balance the need to economize on notation with visual salience of key dependencies. Finally, we note that the implementability constraint ($\sum_{t=0}^{\infty} \beta^t \left[U_{ct}C_t + U_{lt}L_t - U_{ct}G_t^T(T_t)\right] - U_{c0} \left[K_0 \left\{1 + (F_{1k0} - \delta)(1 - \overline{\tau_{k0}})\right\} + B_0\right]$) captures the decentralized behavior of households and firms and is incorporated with Lagrange multiplier ϕ.

A3.1 Proposition 1

In order to derive the optimal carbon price expression of Proposition 1, we first note the following necessary first-order conditions (FOCs) for $t > 0$:
$[C_t]$:

$$
U_{ct} + \phi \left[U_{cct}C_t + U_{ct} + U_{lct}L_t - U_{cct}G_t^T(T_t)\right] = \lambda_{1t} \tag{A1}
$$

Expression (**??**) showcases that the household and the government may differ in their marginal valuation of income (U_{ct} vs. λ_{1t}) if the implementability constraint (IMP) is binding ($\phi > 0$). A wedge between U_{ct} and λ_{1t} also implies that the $MCF_t \equiv \lambda_{1t}/U_{ct} \neq 1$. In contrast, if lump-sum taxes were available, the IMP would not be binding ($\phi = 0$) as the planner could arbitrarily subtract from or add to the right-hand side of the implementability constraint (last row in the planner's problem), in which case $(A1)$ would reduce to $U_{ct} = \lambda_{1t}$ and the marginal cost of public funds would be equal to unity.

$[K_{t+1}]$:

$$\lambda_{1t} = \beta[\lambda_{1t+1}(1 - \delta(SLR_{t+1}, \Lambda^{slr}_{t+1})) + \lambda_{kt+1}] \tag{A2}$$

$[K_{1t}]$:

$$\lambda_{1t} Y_{k1t} = \lambda_{kt} \tag{A3}$$

Combining $(A2)$-$(A3)$ and invoking the decentralized equilibrium condition that the marginal product of capital will equal its factor price, $Y_{k1t} = r_t$, we find that the planner trades off present and future consumption based on the intertemporal marginal rate of transformation or the marginal product of capital:

$$\frac{\lambda_{1t}}{\beta\lambda_{1t+1}} = (1 - \delta(SLR_{t+1}, \Lambda^{slr}_{t+1})) + r_t. \tag{A4}$$

Consider next the optimality conditions for climate-related allocations:

$[T_t]$:

$$U_{Tt} - \phi U_{ct}\frac{\partial G^T_t}{\partial T_t} + \lambda_{1t}[\frac{\partial Y_t}{\partial T_t} - \frac{\partial \gamma^c_t}{\partial T_t}] - \sum_{m=0}^{\infty} \beta^m \zeta_{t+m} \frac{\partial SLR_{t+m}}{\partial T_t} = -\xi_t \tag{A5}$$

$[SLR_t]$:

$$\lambda_{1t}\frac{\partial \delta K_t}{\partial SLR_t} = \zeta_t \tag{A6}$$

$[\mu_t]$, after using $E^M_t = (1 - \mu_t)E_t$ and cancelling out E_t terms on both sides:

$$\lambda_{1t}\Theta'_t(\mu_t) = \sum_{j=0}^{\infty} \beta^j (\xi_{t+j}) \frac{\partial T_t}{\partial E^M_t} \tag{A7}$$

Substituting $(A5)$ and $(A6)$ into $(A7)$ and dividing both sides by λ_{1t} yields:

$$\begin{aligned}&\Theta'_t(\mu_t)\\ &= \sum_{j=0}^{\infty} \beta^j \left[\frac{-U_{Tt+j}}{\lambda_{1t}} + \phi\frac{U_{ct+j}}{\lambda_{1t}}\frac{\partial G^T_{t+j}}{\partial T_{t+j}} - \frac{\lambda_{1t+j}}{\lambda_{1t}}[\frac{\partial Y_{t+j}}{\partial T_{t+j}} - \frac{\partial \gamma^c_{t+j}}{\partial T_{t+j}}] + \sum_{m=0}^{\infty} \beta^m \left(\frac{\lambda_{1t+j+m}}{\lambda_{1t}}\frac{\partial \delta K_{t+j+m}}{\partial SLR_{t+j+m}}\right)\frac{\partial SLR_{t+j+m}}{\partial T_{t+j}}\right.\end{aligned}$$

Comparing this expression to the firm's optimality condition for abatement, $\tau_{Et} = \Theta'_t(\mu_t)$, we immediately see that the optimal allocation can be decentralized by a carbon tax set equal to the right-hand side of this expression which captures the present value of marginal damages from another unit of carbon emissions (provided that all other taxes are set appropriately). In order to complete the derivation of the expression in Proposition 1, we further manipulate each component of the marginal damages in ($A8$) as follows:

Utility impacts: Multiplying by U_{ct}/U_{ct} and invoking the definition of the MCF_t yields:

$$\sum_{j=0}^{\infty}\beta^j\left[\frac{-U_{Tt+j}}{\lambda_{1t}}\frac{U_{ct}}{U_{ct}}\right]\frac{\partial T_{t+j}}{\partial E_t^M}=\sum_{j=0}^{\infty}\left(\frac{1}{MCF_t}\right)\underbrace{\left[\frac{-\beta^j U_{Tt+j}}{U_{ct}}\right]}_{\text{Utility Impacts}}\frac{\partial T_{t+j}}{\partial E_t^M} \tag{A9}$$

This result implies that the planner distorts the internalization of climate utility losses when $MCF > 1$. This result is well-known from prior literature. Intuitively, the planner effectively "taxes" the environmental quality consumption good along with all other consumption (which is taxed via the consumption-labor wedge even in our setting where consumption is normalized as nominally untaxed good). More formally, this result arises due to the additional costs that carbon pricing imposes in the presence of distortionary taxes when $MCF > 1$, also known as "tax-interaction" effects (Bovenberg and Goulder 2002). For example, if carbon prices reduces employment, they may exacerbate the welfare costs of labor income taxes. In settings like ours where the intermediate goods taxation result holds for energy inputs (see also derivation of optimal energy tax below), the revenue recycling benefits of carbon pricing are generally not sufficient to compensate for these tax interaction effects. In contrast, climate impacts on production or capital provide an additional benefit by increasing the size of tax bases and thus mitigating distortions from other taxes. They are thus not subject to the MCF discount. See Barrage (2020) for a detailed discussion.

Transfer impacts: Re-arrange ($A1$) to derive an expression for the Lagrange multiplier on the implementability constraint, $\phi = \frac{\lambda_{1t}-U_{ct}}{[U_{cct}C_t+U_{ct}+U_{lct}L_t-U_{cct}G_t^T(T_t)]}$. Substituting into the government transfers marginal damage term, re-arranging, multiplying by U_{ct}/U_{ct}, and invoking the definition of the MCF_t yields the desired expression:

$$\begin{aligned}
&\sum_{j=0}^{\infty}\beta^j\left[\phi\frac{U_{ct+j}}{\lambda_{1t}}\frac{\partial G_{t+j}^T}{\partial T_{t+j}}\right]\frac{\partial T_{t+j}}{\partial E_t^M} \qquad (A10)\\
=&\sum_{j=0}^{\infty}\beta^j\left(\frac{\lambda_{1t}/U_{ct}-U_{ct}/U_{ct}}{\lambda_{1t}/U_{ct}}\right)\left[\frac{\partial G_{t+j}^T}{\partial T_{t+j}}\right]\left(\frac{U_{ct+j}}{[U_{cct}C_t+U_{ct}+U_{lct}L_t-U_{cct}G_t^T(T_t)]}\right)\frac{\partial T_{t+j}}{\partial E_t^M}\\
=&\sum_{j=0}^{\infty}\beta^j\left(\frac{MCF_t-1}{MCF_t}\right)\underbrace{\left[\frac{\partial G_{t+j}^T}{\partial T_{t+j}}\right]}_{\text{Transfer Impacts}}\underbrace{\left(\frac{U_{ct+j}}{[U_{cct}C_t+U_{ct}+U_{lct}L_t-U_{cct}G_t^T(T_t)]}\right)}_{\text{Offer Curve Impacts}}\frac{\partial T_{t+j}}{\partial E_t^M}
\end{aligned}$$

Intuitively, $(A10)$ can be thought of in two ways. On the one hand, if $MCF_t > 1$, then the need for increased transfers due to warming creates welfare costs from raising the requisite funds, adding to the social cost of carbon (ceteris paribus). On the other hand, additional transfer payments also affect households' offer curves and thereby the planner's ability to decentralize the optimal allocation as a competitive equilibrium. Neither mechanism applies in the standard first-best setting.

Output impacts: First, note that the planner's relative valuation of output at times $t+j$ and time t can be expressed as $\frac{\beta^j \lambda_{1t+j}}{\lambda_{1t}} = \frac{\beta\lambda_{1t+1}}{\lambda_{1t}} \frac{\beta\lambda_{t+2}}{\lambda_{1t+1}} \dots \frac{\beta\lambda_{1t+j}}{\lambda_{1t+j-1}}$. Repeatedly substituting in from $(A4)$ and invoking the definition of the market-based discount factor $M_{t,j} = \prod_{m=1}^{j} \frac{1}{(1+r_{t+m}-\delta_{t+m})}$ for $j > 0$ gives the desired result. Intuitively, the results mean that the planner discounts future output losses from warming based on the marginal rate of transformation between present and future consumption via private capital investments:

$$\sum_{j=0}^{\infty} \beta^j \frac{\lambda_{1t+j}}{\lambda_{1t}} \frac{\partial(-Y_{t+j})}{\partial T_{t+j}} \frac{\partial T_{t+j}}{\partial E_t^M} = \sum_{j=0}^{\infty} M_{t,j} \cdot \underbrace{\left[\frac{-\partial Y_{t+j}}{\partial T_{t+j}}\right]}_{\text{Output Impacts}} \cdot \frac{\partial T_{t+j}}{\partial E_t^M} \tag{A11}$$

Government consumption cost impacts: As shown in $(A8)$, the planner discounts future final good losses equally for output losses and increases in government consumption costs. The derivation of the government consumption cost impact expression is thus the same as for output impacts, yielding:

$$\sum_{j=0}^{\infty} \beta^j \frac{\lambda_{1t+j}}{\lambda_{1t}} \frac{\partial \gamma_{t+j}^c}{\partial T_{t+j}} \frac{\partial T_{t+j}}{\partial E_t^M} = \sum_{j=0}^{\infty} M_{t,j} \cdot \underbrace{\left[\frac{\partial \gamma_{t+j}^c}{\partial T_{t+j}}\right]}_{\text{Gov't Cons. Cost Impacts}} \frac{\partial T_{t+j}}{\partial E_t^M} \tag{A12}$$

Sea-level rise impacts: Finally, expression $(A8)$ also shows that the planner discounts future final good losses from sea-level rise equivalently to production and government consumption costs. The same substitutions for $\frac{\lambda_{1t+j+m}}{\lambda_{1t}}$ as above thus also yield the final expression:

$$\sum_{m=0}^{\infty} \beta^m \left(\frac{\lambda_{1t+j+m}}{\lambda_{1t}} \frac{\partial \delta K_{t+j+m}}{\partial SLR_{t+j+m}}\right) \frac{\partial SLR_{t+j+m}}{\partial T_{t+j}} \frac{\partial T_{t+j}}{\partial E_t^M} = \sum_{j=0}^{\infty} \left[\sum_{m=0}^{\infty} M_{t,j+m} \cdot \underbrace{\frac{\partial \delta_{t+j+m} K_{t+j+m}}{\partial SLR_{t+j+m}} \frac{\partial SLR_{t+j+m}}{\partial T_{t+j}}}_{\text{SLR Impacts}}\right] \frac{\partial T_{t+j}}{\partial E_t^M} \tag{A13}$$

Substituting expressions $(A9)$-$(A13)$ into $(A8)$ and, again, comparing to the firm's optimality condition completes the proof.

A3.2 Income Taxes

In order to characterize optimal labor and capital income taxes we first consider the following additional optimality conditions from the planner's problem (for $t > 0$):

$[L_t]$:

$$-U_{lt} - \phi[U_{clt}C_t + U_{lt} + U_{llt}L_t - U_{clt}G_t^T(T_t)] = \lambda_{lt} \tag{A14}$$

$[L_{1t}]$:

$$\lambda_{1t}Y_{l1t} = \lambda_{lt} \tag{A15}$$

To save on notation, let $\Delta_t^l \equiv U_{clt}C_t + U_{lt} + U_{llt}L - U_{clt}G_t^T(T_t)$ in $(A14)$ and define the analogous term from the optimality condition for consumption $(A1)$ as $\Delta_t^c \equiv U_{cct}C_t + U_{ct} + U_{lct}L_t - U_{cct}G_t^T(T_t)$. In the decentralized equilibrium, the marginal product of labor equals the wage, $Y_{L1t} = w_t$. Substituting into $(A15)$, combining $(A1)$, $(A14)$, and $(A15)$, and comparing with the household's optimality condition, $\frac{-U_{lt}}{U_{ct}} = w_t(1 - \tau_{lt})$, yields the following implicit expression for the net-of-labor tax rate:

$$(1 - \tau_{lt}^*) = \frac{1 + \phi\Delta_t^c/U_{ct}}{1 + \phi\Delta_t^l/U_{lt}} \tag{A16}$$

In the broader literature, one can often draw additional inference on optimal labor wedges with certain restrictions on preferences. For example, if $U(C_t, L_t; T_t, \Lambda_t^u) = \frac{C_t^{1-\sigma}}{1-\sigma} - \theta\ln(L_t) + h(T_t(1 - \Lambda_t^u))$, then Δ_t^c/U_{ct} simplifies to $1 - \sigma + \sigma\frac{G_t^T(T_t)}{C_t}$ and $\Delta_t^l/U_{lt} = 0$ so that, for $t > 0$:

$$(1 - \tau_{lt}^*) = 1 + \phi(1 - \sigma) + \phi\sigma\frac{G_t^T(T_t)}{C_t} \tag{A17}$$

In a setting without government transfers or where transfers are a constant fraction of consumption, $(A16)$ would thus indicate the desirability of a constant labor wedge. In the present setting, in contrast, such inference is complicated by the effects of warming on public transfers.[15]

To characterize optimal intertemporal wedges, we compare $(A4)$ to the household's intertemporal optimality condition at equilibrium prices (where $r_{t+1} = Y_{K_{t+1}}$) :

$$\frac{U_{ct}}{\beta U_{ct+1}} = \left\{1 + (r_{t+1} - \delta(SLR_{t+1}, \Lambda_{t+1}^{slr}))(1 - \tau_{kt+1})\right\} \tag{A18}$$

[15] There is, of course, a caveat that the level of transfers absent climate change is taken as given in our setting. In a representative agent economy without micro-foundations for various transfer programs such as unemployment insurance or Social Security, this is a somewhat inevitable simplification. It does, however, imply that the optimal fiscal response to climate change may look different in an economy with such micro-foundations where transfer program generosity and tax rates may be simultaneously optimized.

This comparison shows that the desirability of zero capital income taxes requires that:

$$\frac{U_{ct}}{\beta U_{ct+1}} = \frac{\lambda_{1t}}{\beta \lambda_{1t+1}} = \frac{U_{ct} + \phi \Delta_t^c}{\beta \left(U_{ct+1} + \phi \Delta_{t+1}^c \right)} \tag{A19}$$

As before, there are well-known utility functions for which $(A19)$ holds *if* one further imposes appropriate restrictions on $\frac{G_t^T(T_t)}{C_t}$, such that it is equal to a constant fraction of consumption. On the other hand, however, the calibration of the COMET does not match these assumptions exactly, so that capital income taxes are not always optimally zero.

A3.3 Proposition 2

Part 1 follows from the social planner's FOC for utility adaptation spending γ_t^u for $t > 0$:

$$U_{\Lambda_t^u} f_{\gamma_t^u}^u = \lambda_{1t}$$

Multiplying by U_{ct}/U_{ct}, re-arranging, and invoking the definition of the MCF_t yields the desired expression:

$$\frac{U_{\Lambda_t^u}}{U_{ct}} \frac{1}{MCF_t} = \frac{1}{f_{\gamma_t^u}^u} \tag{A20}$$

Part 2 similarly follows directly from the FOC for production adaptation spending γ_t^y for $t > 0$:

$$\frac{\partial Y_t}{\partial \Lambda_t^y} = \frac{1}{f_{\gamma_t^y}^y} \tag{A21}$$

The difference between allocation rules $(A20)$ and $(A21)$ can be thought of as follows. On the one hand, if taxes are distortionary and $MCF > 1$, the costs of providing public goods is generally higher. Whether the planner should therefore reduce the provision (relatively) of these goods in general equilibrium, however, also depends on how their provision affects public finances. In our setting, public protection against climate production damages yields an additional fiscal benefit through higher marginal products of capital and labor, increasing the economy's tax base, ceteris paribus. More formally, both the costs and benefits of γ_t^y arise from changes in final good availability, so that their comparison by the planner is not affected by potential wedges between the planner's and the household's respective valuations of the final good. For the public provision of utility protection, in contrast, a wedge applies since utility adaptation provides no additional fiscal benefits.

Finally, Part 3 follows from the FOCs for sea-level rise adaptation:

$[\Gamma_{t+1}]$:

$$\beta \eta_{St+1} f_{\Gamma_{t+1}}^{slr} + \beta \eta_{\Gamma t+1} (1 - \delta^\Gamma) = \eta_{\Gamma t} \tag{A22}$$

$[\gamma_t^{slr}]$:

$$\lambda_{1t} = \eta_{\Gamma t} \tag{A23}$$

$[\Lambda_t^{SLR}]$:

$$\lambda_{1t} \frac{-\partial \delta}{\partial \Lambda_t^{slr}} K_t = \eta_{St} \tag{A24}$$

Combining $(A22)$-$(A24)$ yields the desired optimality condition. Intuitively, it shows that the planner equates the returns to investing in adaptation capital - given by the avoided capital losses net of depreciation - to the equilibrium return on private capital:

$$\frac{-\partial \delta}{\partial \Lambda_{t+1}^{slr}} f_{\Gamma_{t+1}}^{slr} K_{t+1} + (1 - \delta^{\Gamma}) = \frac{\lambda_{1t}}{\beta \lambda_{1t+1}}$$

A4 Further Calibration Details

A4.1 Baseline Government Expenditures

Absent climate change, U.S. government expenditures are projected to increase at the rates of population growth g_t^{Pop} and productivity growth g_t^{TFP}, plus an additional adjustment for healthcare g_t^H to reflect rising relative costs. Formally, baseline expenditures follow:

$$\begin{aligned} \overline{\gamma_t^{c,nh}} &= \overline{\gamma_{t-1}^{c,nh}} \cdot (1 + g_t^{Pop} + g_t^{TFP}) \\ \overline{\gamma_t^{c,h}} &= \overline{\gamma_{t-1}^{c,h}} \cdot (1 + g_t^{Pop} + g_t^{TFP} + g_t^{H}) \\ \overline{G_t^T} &= \overline{G_{t-1}^T} \cdot (1 + g_t^{Pop} + g_t^{TFP}) \end{aligned} \tag{A25}$$

with initial values set to observed 2025 levels. Empirically, this approach performs very well for long-run projections. Figure A8 compares the actual evolution of real ($2017) U.S. government consumption expenditures from 1970-2023 with a "projection" that starts with observed 1970 values and predicts forward based on $(A25)$ using only data on real TFP growth from the Penn World Tables (PWT 11.0, October 2025 release, Feenstra et al. 2015) and population growth from FRED (Federal Reserve Bank of St. Louis). The figure shows that, while there are of course cyclical and political fluctuations in government spending, central long-run movement in U.S. government consumption is historically well-captured by $(A25)$.

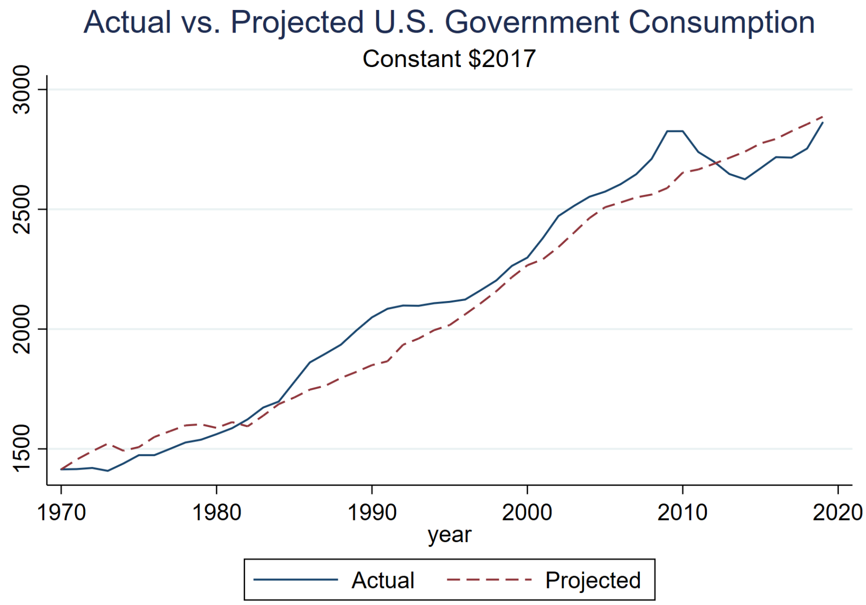

Figure A8: Actual vs. predicted U.S. government consumption

A4.2 Sea Level Rise Costs

Figure A9 shows estimated gross sea level rise damages (EPA 2017) plotted against corresponding median global sea level rise values (Kopp et al. 2017).

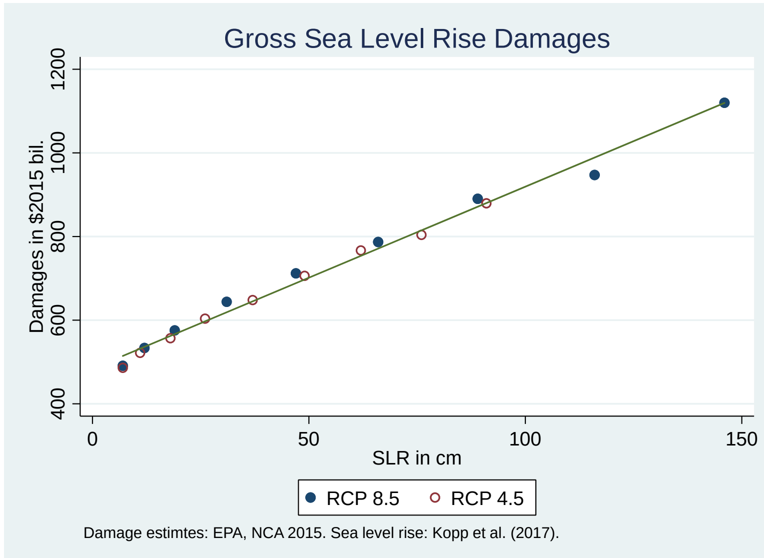

Figure A9: Gross U.S. sea level rise costs and global sea level rise levels

A4.3 Clean Energy Costs

The production of clean energy requires extra costs $\Theta_t(\mu_t)E_t$ which we quantify based on the DICE-2023 model. First, we posit that $\Theta_t(\mu_t) = b_{1t}(\mu_t)^{b_2}$. Second, we adopt the convexity parameter $b_2 = 2.6$. Third, we set b_{1t} such that the marginal abatement costs at $\mu_t = 1$ (full abatement) match the DICE-2023 estimates of the (average marginal) backstop technology cost at each time via $MC_t(\mu_t = 1) = b_{1t}b_2(1)^{b_2-1} = pbackstop_t$. We do, however, also maintain the assumption of the older DICE vintages that abatement costs at some point fall to zero, and set this time to 2225 (after the direct optimization period).

A4.4 Carbon Cycle and Climate System

The carbon cycle model builds on the DFAIR implementation of the FAIR model (Millar et al. 2017) in Barrage and Nordhaus (2024), with one adjustment for the model time step and one simplification that aids computation but leaves temperature projections virtually unaffected, as described below. There are four (excess) carbon reservoirs, indexed by i, with respective content levels $R_{i,t}$ at time t. For ease of exposition, t here refers to calendar rather than model years. Atmospheric carbon concentrations in GtC, MAT_t, are given by:

$$MAT_t = MAT_{1765} + \sum R_{i,t}$$

The reservoirs' concentrations evolve according to:

$$R_{i,t} = a_i \tau_i \alpha_t [\frac{E_t^M + E_t^{M,ROW}}{\Delta}](1 - \exp(\frac{-\Delta}{\alpha_t \tau_i})) + R_{i,t-1} \exp(\frac{-\Delta}{\alpha_t \tau_i})$$

where Δ denotes the size of the time step in years, a_i and τ_i are parameters, and α_t is a saturation variable that evolves as a function of cumulative carbon emissions and temperature change. That is, the predicted 100 year integrated impulse response function $iIRF_{100,t}$ at time t is given by

$$iIRF_{100,t} = irf_0 + irf_C C_{acc,t} + irf_T T_t$$

where the $r's$ are parameters, T_t is mean atmospheric global temperature change over pre-industrial levels, and $C_{acc,t}$ is accumulated carbon outside the atmosphere defined by

$$C_{acc,t} = \sum_{v=1765}^{t} [E_v^M + E_v^{M,ROW}] - [MAT_t - MAT_{1765}].$$

While (D)FAIR solves numerically for α_t at each time step based on an implicit equation for $IRF_{100,t}$, to ease computation we estimate the following lagged approximation (using estimated values from the base scenario in DICE-2023):

$$\widehat{\alpha}_t = (0.010374981) \cdot e^{0.0884138 * IRF_{100,t-1}} \tag{A26}$$

Testing $(A26)$ within DICE-2023 reveals that the projected temperature changes through 2300 are almost indistinguishable from those obtained in the original model.

The increase in radiative forcing at time t in w/m^2, $FORC_t$, depends on carbon concentrations and exogenous forcings $FORC_t^{EX}$ via:

$$FORC_t = \frac{F_{2x}}{\ln(2)} \ln\left(\frac{MAT_t}{MAT_{1765}}\right) + FORC_t^{EX}$$

While DICE-2023 endogenizes mitigation of some non-CO_2 forcings, we abstract from this feature and maintain non-CO_2 forcings as exogenous and quantify them as in the DICE-2016 model (Nordhaus, 2017). Finally, the climate system is represented by two temperature boxes and modeled here exactly as in DICE-2023:

$$\begin{aligned} Tbox_{j,t+1} &= Tbox_{j,t} \cdot e^{-\Delta/d_j} + teq_j \cdot FORC_{t+1}[1 - e^{-\Delta/d_j}] \text{ for } j \in \{1,2\} \\ T_t &= Tbox_{1,t} + Tbox_{2,t} \end{aligned}$$

The parameter values and initial conditions used are as follows: $MAT_{1765} = 588$ GtC; $MAT_{2020} =$

886.5; a_0 = 0.2173; a_1 =0.224; a_2 =0.2824; a_3 =0.2763; τ_0 = 1000000; τ_1 = 394.4; τ_2 = 36.53; τ_3 = 4.304; $R_{0,2020}$ = 150.093; $R_{1,2020}$ = 102.698; $R_{2,2020}$ = 39.534; $R_{3,2020}$ =6.1865; α_{2020} = 0.44715; $\sum\limits_{v=1765}^{2020}[E_v^M + E_v^{M,ROW}]$ = 633.5 GtC; irf_0 =32.4; irf_C = 0.019; irf_T = 4.165; F_{2x} =3.93; $FORC_{2020}^{EX}$ = 0.7240; $FORC_{2100}^{EX}$ = 0.30; $Tbox_{1,2020}$ = 0.1477 ; $Tbox_{2,2020}$ = 1.099454; teq_1 = 0.324; teq_2 = 0.44; d_1 = 236; d_2 = 4.07.

A4.5 Calibration Summary

The following table summarizes the calibration parameters in the benchmark scenario (besides the climate module parameters already summarized above). This scenario assumes optimized distortionary taxes and moderate production and utility damages. Parameter values in alternate scenarios are provided in the replication files. We note that many parameters are interdependent and also vary with the fiscal scenario such as due to the fact that initial labor supply is rationalized at different assumed tax rates. The table uses "0" to denote the model base year of 2025. We also note that the model is calibrated in \$2016 but the results are presented in \$2025 which we convert using the U.S. GDP deflator from FRED (2017 base year, chained).

Table A9: Benchmark Economic Calibration Parameters		
Parameter	**Value**	**Sources and Notes**
Preferences: $U(c_t, l_t, T_t) = \frac{[c_t \cdot (1-\varsigma l_t)^{\gamma}]^{1-\sigma}}{1-\sigma} + \frac{\left(1+\alpha_u T_t^2\right)^{-(1-\sigma)}}{1-\sigma}$		
σ	1.5	Barrage (2020)
β	$(.985)^{10}$	Barrage (2020)
ς	0.6716 if distortionary	Jointly match Frisch elasticity (0.78) and rationalize base labor supply ($l_0 = .2324$) at base year marginal product of labor w_0 with $\tau_{l,0}$= 0.35 or $\tau_{l,0}$= 0.0 , resp.
γ	2.2014 if distortionary	
α_u	$9.0636e^{-7}$ if distortionary	Match disutility from equiv. to 50% of output loss in damage scenario
Production Damages: $(1 - D_t(T_t)) = \frac{1}{1+\theta_1 T_t^2}$		
θ_1	0.00069, 0.0011, 0.0017	Match 1.25%, 2%, or 3% annual loss at 4.3°C.
Final Goods Production: $F_1(A_{1t}, T_t, L_{1t}, K_{1t}, E_t) = (1 - \widehat{D}(T_t))A_{1t}(K_{1t}^{\alpha} L_{1t}^{1-\alpha-v} E_t^v)$		
α	0.3	GHKT (2014)
v	0.03	GHKT (2014)
K_0	4.8556e+04	$= \frac{\alpha \cdot GDP_{2025}}{(r+\delta^{Yr})} = \frac{\alpha \cdot GDP_{2015}}{(.05+.10)}$ ($2016 billions)
$\pi_{1,0}^l$	.9823	Base year share of labor in final goods sector
		$=\frac{1-\alpha-v}{\alpha_E v+1-\alpha-v}$ (equates $MPL_{1,0}$=$MPL_{E,0}$)
$\pi_{1,0}^k$	0.9437	Base year share of capital in final goods sector
		$=\frac{\alpha}{(1-\alpha_E)v+\alpha}$ (equates $MPK_{1,0}$=$MPK_{E,0}$)
E_0	1.3362	EIA (2026) (GtC/year)
l_0	.2324	OECD (2020) (fraction of time supplied as labor)
$A_{1,0}$	5.5263e+04	$= \frac{(10 \cdot GDP_0)}{(1-D(T_0))K_{1,0}^{\alpha}(l_0 \cdot \pi_{1,0}^l \cdot N_0)^{1-\alpha-v}(10 \cdot E_0)^v}$
$A_{1,t}$	$= A_{1,t-1} \cdot \frac{1}{1-gA_{1,t-1}}$	for $t \geq 2035$
$\overline{\delta}$	0.6513	Match annual δ^{Yr} = 10% (in % per decade)
Energy Good Production: $E_t = A_{2t}(K_{2t}^{1-\alpha_E} L_{2t}^{\alpha_E})$		
α_E	0.403	U.S. Bureau of Economic Analysis Data (2000-10)
$K_{2,0}$	2.7355e+03	$= (1 - \pi_{1,0}^k)K_0$ ($2016 billions)
- Continued on next page -		

Table A9: Benchmark Economic Calibration Parameters		
Parameter	**Value**	**Sources and Notes**
$A_{2,0}$	1.7717	$= \frac{E_0 \cdot 10}{(K_{E,0})^{(1-\alpha_E)}(l_0(1-\pi^l_{1,0})N_0)^{\alpha_E}}$
$A_{2,t}$	$=A_{2,t-1} \cdot (1+gZ_{t-1})^{\alpha_E}$	Note: gZ_{t-1} is *labor* productivity growth (see below)
Government:		
$\tau_{l,0}$	$\begin{cases} 35\% & \text{if distortionary} \end{cases}$	Avg. effective rate (OECD; Carey and Tchilinguirian 2000)
$\tau_{k,0}$	$\begin{cases} 29.0\% & \text{if distortionary} \end{cases}$	Avg. effective rate (CBO 2014)
$\gamma_0^{c,nh}$	3,173 \$2016 billion	Gov't Consumption Expenditures (NIPA 2026)
$\gamma_0^{c,h}$	1,950 \$2016 billion	Health expenditures (CMS 2026, data for 2024)
G_0^T	1,865 \$2016 billion	Transfers (NIPA 2026) - Health expenditures (CMS)
gH_t	$\begin{cases} (0.01623 \cdot 10) & \text{if } t \preceq 2055 \\ 0 & \text{o.w.} \end{cases}$	Annualized estimates in health cost growth from CBO (2021)
B_0/GDP_0	66.76%	Federal debt held by domestic public (FRED, CRS)
Abatement Costs: $\Theta_t(\mu_t) = b_{1,t}(\mu_t)^{b_2}$		
b_2	2.6	Barrage and Nordhaus (2024)
$P_t^{backstop}$	2352; 2128; 1925; ... $= 0$ after 2225	(\$2016/tC) Barrage and Nordhaus (2024), FRED
$b_{1,0}$	904.518	$=P_0^{\text{Backstop}} / b_2$
Sea Level Rise Impacts: $\delta(SLR_t, \Lambda_t^{slr}) = \overline{\delta} + \delta^{SLR} \cdot SLR_t \cdot (1-\Lambda_t^{slr})$		
δ^{SLR}	0.000186	Estimated from EPA Coastal Property Model (EPA 2017)
Sea Level Rise Adaptation: $\Lambda_t^{slr} = \left(\gamma_1 \Gamma_t / (\delta^{SLR} \cdot SLR_t \cdot K_t)\right)^{\gamma_2}$; $\Gamma_t = \Gamma_{t-1}(1-\delta^{\Gamma}) + \gamma_t^{SLR}$		
ι_1, ι_2	10.7965, 0.0840	Minimize sum of squared deviations between model
δ^{Γ}	0.2780	and EPA Coastal Property Model results (EPA 2017)
Miscellaneous:		
N_0	0.342	U.S. Census (billions)
g_t^{Pop}	varies over time	U.S. value from RICE (Nordhaus 2010)
g_t^{TFP}	varies over time	U.S. value from RICE (Nordhaus 2010)

A5 Further Modeling Results

Figure A10 shows a variant of Figure 4 that illustrates each cost impact channel's contribution as a share of the total rather than in levels. The shares are broadly stable, though healthcare and labor tax losses rise over time in their significance.

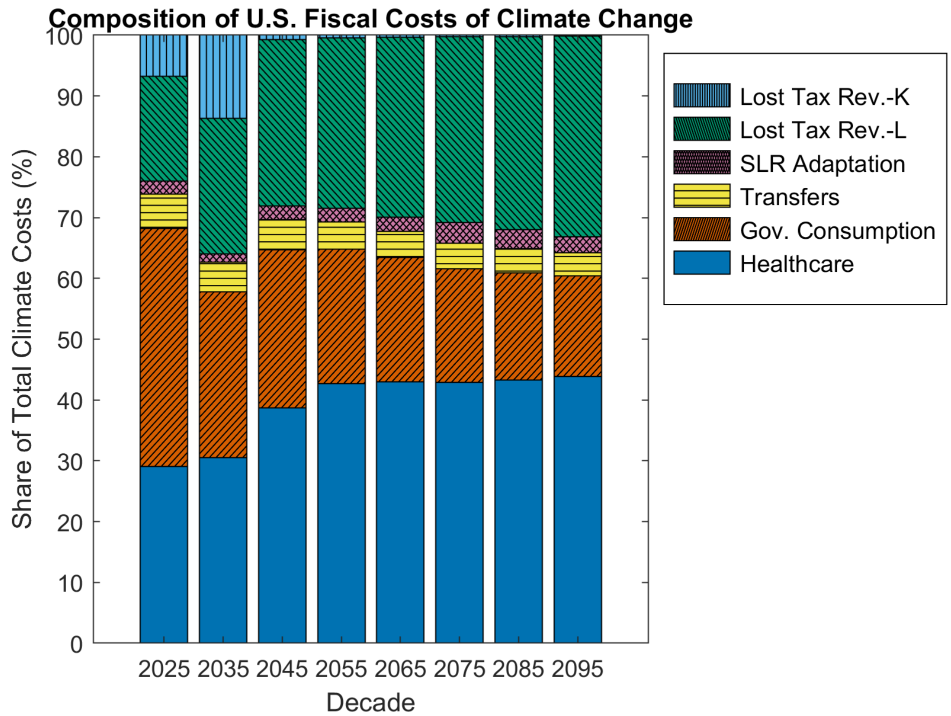

Figure A10: Proportional contribution of different climate fiscal cost mechanisms over time in the benchmark scenario

References

[1] Anthoff, David, and Richard S.J. Tol. "The Climate Framework for Uncertainty, Negotiation and Distribution (FUND), Technical Description, Version 3.9." (2014). URL accessed August 2025): [https://www.fund-model.org/files/documentation/Fund-3-9-Scientific-Documentation.pdf]

[2] Bakkensen, Laura, and Lint Barrage. "Climate shocks, cyclones, and economic growth: bridging the micro-macro gap." *The Economic Journal* 136(673): 279-310. 2026.

[3] Bakkensen, Laura A., and Robert O. Mendelsohn. "Risk and adaptation: Evidence from global hurricane damages and fatalities." Journal of the Association of Environmental and Resource Economists 3, no. 3 (2016): 555-587.

[4] Barrage, Lint "Optimal dynamic carbon taxes in a climate-economy model with distortionary fiscal policy." *The Review of Economic Studies,* 87(1): 1-39. (2020).

[5] Barrage, Lint, and William Nordhaus. "Policies, Projections, and the Social Cost of Carbon: Results from the DICE-2023 Model." *Proceedings of the National Academy of Sciences*121, no. 13 (2024): e2312030121.

[6] Boomhower, Judson, Meredith Fowlie, Jacob Gellman, and Andrew Plantinga. How Are Insurance Markets Adapting to Climate Change? Risk Classification and Pricing in the Market for Homeowners Insurance. No. w32625. National Bureau of Economic Research, 2024.

[7] Bovenberg, Lans A., and Lawrence H. Goulder (2002) "Environmental Taxation and Regulation" Chapter 23 in: Alan J. Auerbach and Martin Feldstein (eds.) *Handbook of Public Economics*, Elsevier, Volume 3, Pages 1471-1545.

[8] California Department of Insurance (CDI). "Bulletin 2025-4." URL (accessed August 2025): [https://www.insurance.ca.gov/0250-insurers/0300-insurers/0200-bulletins/bulletin-notices-commiss-opinion/upload/Bulletin-2025-4-Updated-Guidance-regarding-Insurer-Recoupment-Procedures-in-Response-to-Assessment-by-the-FAIR-Plan.pdf]

[9] Carey, David, and Harry Tchilinguirian. "Average effective tax rates on capital, labour and consumption." OECD, https://doi.org/10.1787/247874530426. (2000).

[10] Carleton, Tamma, Amir Jina, Michael Delgado, Michael Greenstone, Trevor Houser, Solomon Hsiang, Andrew Hultgren et al. "Valuing the global mortality consequences of climate change accounting for adaptation costs and benefits." *The Quarterly Journal of Economics* 137, no. 4 (2022): 2037-2105.

[11] Colin Cameron, A., and Douglas L. Miller. "A practitioner's guide to cluster-robust inference." *Journal of Human Resources* 50, no. 2 (2015): 317-372.

[12] Congressional Budget Office (CBO). "Long-Term Budget Projections" March (2021), URL [https://www.cbo.gov/about/products/budget-economic-data#1]

[13] Congressional Budget Office (CBO). "Potential Increases in Hurricane Damage in the United States: Implications for the Federal Budget" Publication 51518 (2016).

[14] Congressional Budget Office (CBO). "Taxing Capital Income: Effective Marginal Tax Rates Under 2014 Law and Selected Policy Options" December 2014.

[15] Congressional Research Service (CRS). "National Flood Insurance Program Borrowing Authority." CRS Report IN10784. (2025). URL (accessed August 2025): [https://sgp.fas.org/crs/homesec/IN10784.pdf]

[16] Correia, Sergio, Paulo Guimarães, and Tom Zylkin. "Fast Poisson estimation with high-dimensional fixed effects." The Stata Journal 20, no. 1 (2020): 95-115.

[17] Deschênes, Olivier, and Michael Greenstone. "Climate change, mortality, and adaptation: Evidence from annual fluctuations in weather in the US." American Economic Journal: Applied Economics 3, no. 4 (2011): 152-185.

[18] Drescher, Katharina, and Benedikt Janzen. "When weather wounds workers: The impact of temperature on workplace accidents." Journal of Public Economics 241 (2025): 105258.

[19] Emanuel, Kerry A. "Downscaling CMIP5 climate models shows increased tropical cyclone activity over the 21st century." Proceedings of the National Academy of Sciences 110, no. 30 (2013): 12219-12224.

[20] Emmerling, Johannes, Laurent Drouet, Lara Aleluia Reis, Michela Bevione, Loic Berger, Valentina Bosetti, Samuel Carrara et al. The WITCH 2016 model-documentation and implementation of the shared socioeconomic pathways. No. 42.2016. Nota di Lavoro, 2016.

[21] Environmental Protection Agency (EPA). 2017. Multi-Model Framework for Quantitative Sectoral Impacts Analysis: A Technical Report for the Fourth National Climate Assessment. U.S. Environmental Protection Agency, EPA 430-R-17-001.

[22] Feenstra, Robert C., Robert Inklaar, and Marcel P. Timmer. "The next generation of the Penn World Table." American economic review 105, no. 10 (2015): 3150-3182.

[23] Garcia-Menendez, F., R. Saari, E. Monier, N. Selin. 2015. "U.S. Air Quality and Health Benefits from Avoided Climate Change under Greenhouse Gas Mitigation." *Environmental Science & Technology* 49 (13), 7580-7588.

[24] Gergel, Diana R., Steven B. Malevich, Kelly E. McCusker, Emile Tenezakis, Michael T. Delgado, Meredith A. Fish, and Robert E. Kopp. "Global Downscaled Projections for Climate Impacts Research (GDPCIR): preserving quantile trends for modeling future climate impacts." *Geoscientific Model Development* 17, no. 1 (2024): 191-227.

[25] Golosov, Mikhail, John Hassler, Per Krusell, and Aleh Tsyvinski. "Optimal taxes on fossil fuel in general equilibrium." *Econometrica* 82, no. 1 (2014): 41-88.

[26] Gould, Carlos F., Sam Heft-Neal, Alexandra K. Heaney, Eran Bendavid, Christopher W. Callahan, Mathew V. Kiang, Josh Graff Zivin, and Marshall Burke. "Temperature extremes impact mortality and morbidity differently." *Science Advances* 11, no. 31 (2025): eadr3070.

[27] Heutel, Garth, Nolan H. Miller, and David Molitor. "Adaptation and the mortality effects of temperature across US climate regions." *Review of Economics and Statistics* 103, no. 4 (2021): 740-753.

[28] Hsiang, Solomon, Robert Kopp, Amir Jina, James Rising, Michael Delgado, Shashank Mohan, D. J. Rasmussen et al. "Estimating economic damage from climate change in the United States." *Science* 356, no. 6345 (2017): 1362-1369.

[29] Hsiang, Solomon M., and Daiju Narita. "Adaptation to cyclone risk: Evidence from the global cross-section." Climate Change Economics 3, no. 02 (2012): 1250011.

[30] Karlsson, Martin, and Nicolas R. Ziebarth. "Population health effects and health-related costs of extreme temperatures: Comprehensive evidence from Germany." *Journal of Environmental Economics and Management* 91 (2018): 93-117.

[31] Knutson, Thomas R., Joseph J. Sirutis, Gabriel A. Vecchi, Stephen Garner, Ming Zhao, Hyeong-Seog Kim, Morris Bender, Robert E. Tuleya, Isaac M. Held, and Gabriele Villarini. "Dynamical downscaling projections of twenty-first-century Atlantic hurricane activity: CMIP3 and CMIP5 model-based scenarios." Journal of Climate 26, no. 17 (2013): 6591-6617.

[32] Kopp, Robert E., Robert M. DeConto, Daniel A. Bader, Carling C. Hay, Radley M. Horton, Scott Kulp, Michael Oppenheimer, David Pollard, and Benjamin H. Strauss. "Evolving understanding of Antarctic ice-sheet physics and ambiguity in probabilistic sea-level projections." Earth's Future 5, no. 12 (2017): 1217-1233.

[33] Kopp, Robert E., Radley M. Horton, Christopher M. Little, Jerry X. Mitrovica, Michael Oppenheimer, D. J. Rasmussen, Benjamin H. Strauss, and Claudia Tebaldi. "Probabilistic 21st and 22nd century sea-level projections at a global network of tide-gauge sites." Earth's future 2, no. 8 (2014): 383-406.

[34] Larsen, Bradley J., Timothy J. Ryan, Steven Greene, Marc J. Hetherington, Rahsaan Maxwell, and Steven Tadelis. "Counter-stereotypical messaging and partisan cues: Moving the needle on vaccines in a polarized United States." *Science advances* 9, no. 29 (2023): eadg9434.

[35] Lee, Jangho, and Andrew E. Dessler. "Future temperature-related deaths in the US: The impact of climate change, demographics, and adaptation." GeoHealth 7, no. 8 (2023): e2023GH000799.

[36] Meinshausen, M., S. C. B. Raper and T. M. L. Wigley (2011). "Emulating coupled atmosphere-ocean and carbon cycle models with a simpler model, MAGICC6: Part I –

Model Description and Calibration." *Atmospheric Chemistry and Physics* 11: 1417-1456. doi:10.5194/acp-11-1417-2011

[37] Millar, Richard J., Zebedee R. Nicholls, Pierre Friedlingstein, and Myles R. Allen. "A modified impulse-response representation of the global near-surface air temperature and atmospheric concentration response to carbon dioxide emissions." *Atmospheric Chemistry and Physics* 17, no. 11 (2017): 7213-7228.

[38] Mullins, Jamie T., and Corey White. "Temperature and mental health: Evidence from the spectrum of mental health outcomes." *Journal of Health Economics* 68 (2019): 102240.

[39] Nordhaus, William D. "Revisiting the social cost of carbon." *Proceedings of the National Academy of Sciences* 114, no. 7 (2017): 1518-1523.

[40] Nordhaus, William D. "Economic aspects of global warming in a post-Copenhagen environment." *Proceedings of the National Academy of Sciences* 107, no. 26 (2010): 11721-11726.

[41] Office of Management and Budget (OMB). "Climate Change: The Fiscal Risks Facing the Federal Government" November 2016. URL (accessed November 2019): [https://obamawhitehouse.archives.gov/sites/default/files/omb/reports/omb_climate_change_fiscal_ri

[42] Rasmussen, D. J., Malte Meinshausen, and Robert E. Kopp. "Probability-weighted ensembles of US county-level climate projections for climate risk analysis." *Journal of Applied Meteorology and Climatology* 55, no. 10 (2016): 2301-2322.

[43] Rennert, Kevin, Frank Errickson, Brian C. Prest, Lisa Rennels, Richard G. Newell, William Pizer, Cora Kingdon et al. "Comprehensive evidence implies a higher social cost of CO2." *Nature* 610, no. 7933 (2022): 687-692.

[44] Rizmie, Dheeya, Laure de Preux, Marisa Miraldo, and Rifat Atun. "Impact of extreme temperatures on emergency hospital admissions by age and socio-economic deprivation in England." Social Science & Medicine 308 (2022): 115193.

[45] Rode, Ashwin, Tamma Carleton, Michael Delgado, Michael Greenstone, Trevor Houser, Solomon Hsiang, Andrew Hultgren et al. "Estimating a social cost of carbon for global energy consumption." *Nature* 598, no. 7880 (2021): 308-314.

[46] Somanathan, Eswaran, Rohini Somanathan, Anant Sudarshan, and Meenu Tewari. "The impact of temperature on productivity and labor supply: Evidence from Indian manufacturing." Journal of political Economy 129, no. 6 (2021): 1797-1827.

[47] Tebaldi, Claudia, Kevin Debeire, Veronika Eyring, Erich Fischer, John Fyfe, Pierre Friedlingstein, Reto Knutti et al. "Climate model projections from the scenario model intercomparison project (ScenarioMIP) of CMIP6." *Earth System Dynamics* 12(1): 253-293 (2021).

[48] Tol, Richard SJ, and Hadi Dowlatabadi. "Vector-borne diseases, development & climate change." Integrated Assessment 2, no. 4 (2001): 173-181.

[49] U.S. Forest Service (2016) "Climate Change & Fiscal Risk: Wildland Fire Technical Supplement" URL (last accessed January 2024): [https://obamawhitehouse.archives.gov/sites/default/files/omb/assets/techdocs/Wildland%20Fire%20T

[50] White, Corey. "The dynamic relationship between temperature and morbidity." *Journal of the Association of Environmental and Resource Economists* 4, no. 4 (2017): 1155-1198.